Radio source evolution

Manel Perucho Pla

Departament d'Astronomia i Astrofísica

Observatori Astronòmic

Universitat de València

Great to be back

Outline

- The inner kiloparsec:
  - Deceleration mechanisms.
- Beyond the inner kiloparsec:
  - Evolution of powerful radio sources.
- Conclusions.

Radio source evolution

The inner kiloparsec: Deceleration mechanisms

Radio-source evolution

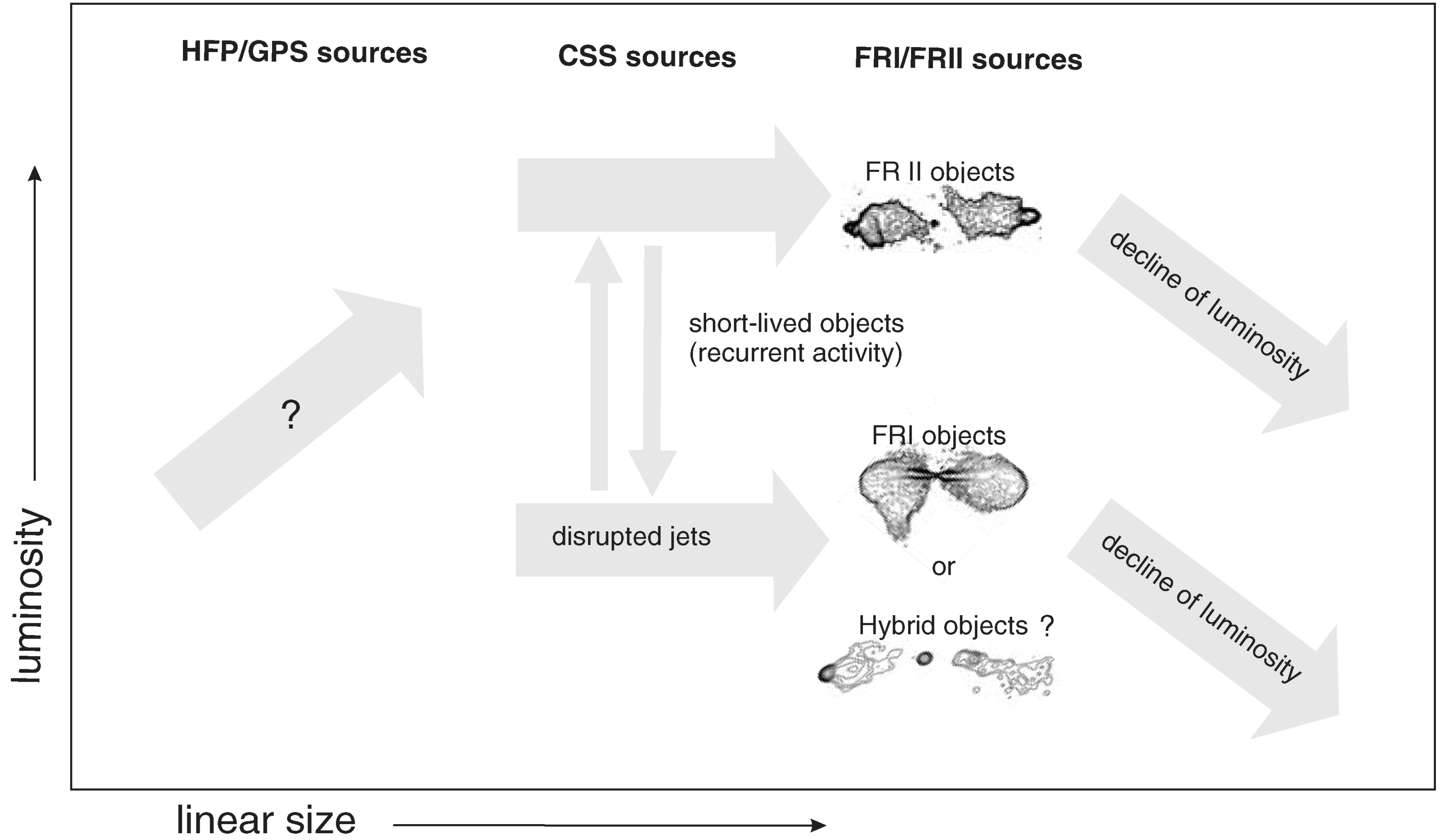

From Kunert-Bajraszewska et al. (2010)

Homogeneous versus clumpy medium

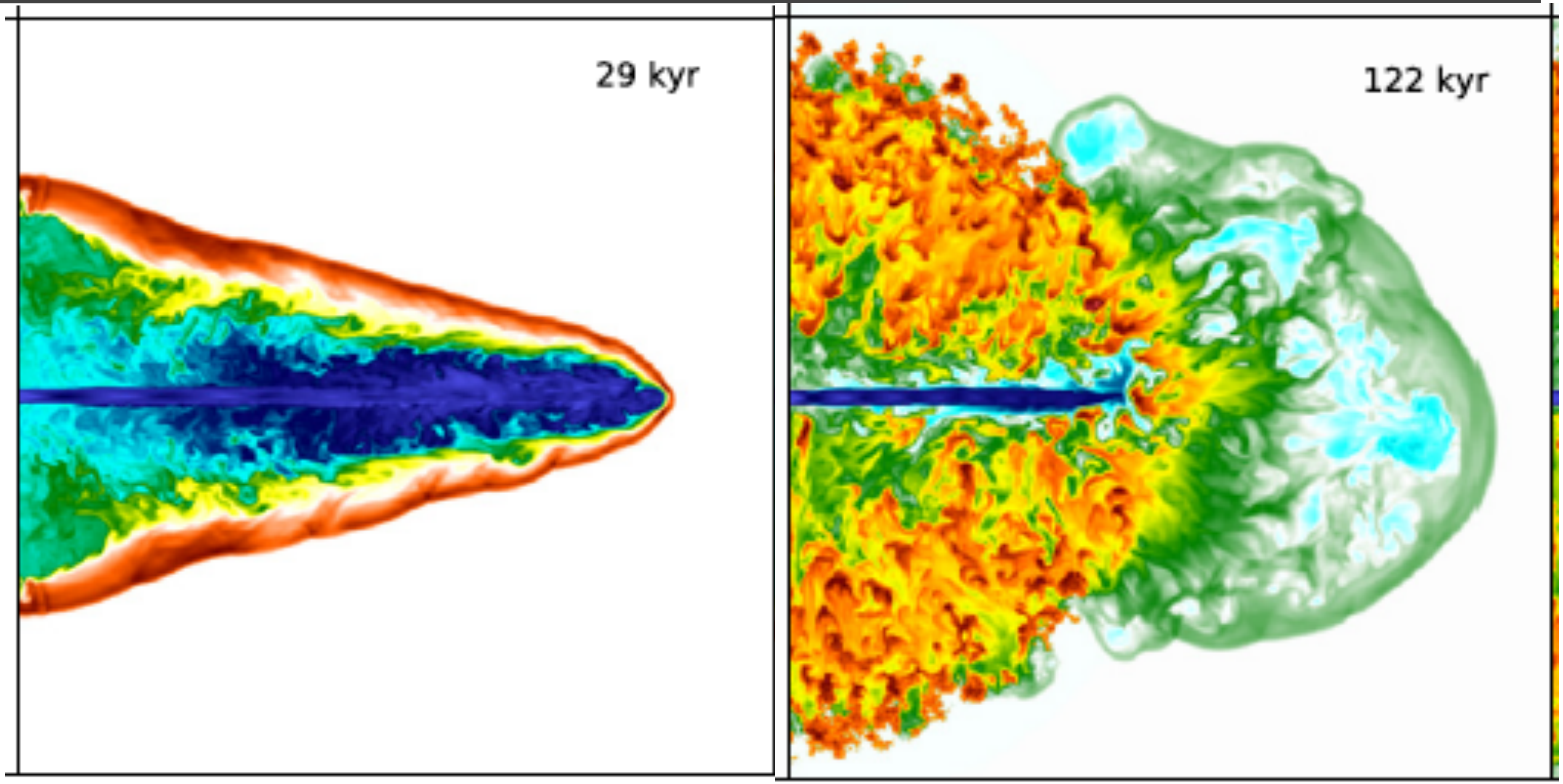

Wagner & Bicknell (2011)
Wagner et al. (2012)

Correlation with star-formation?

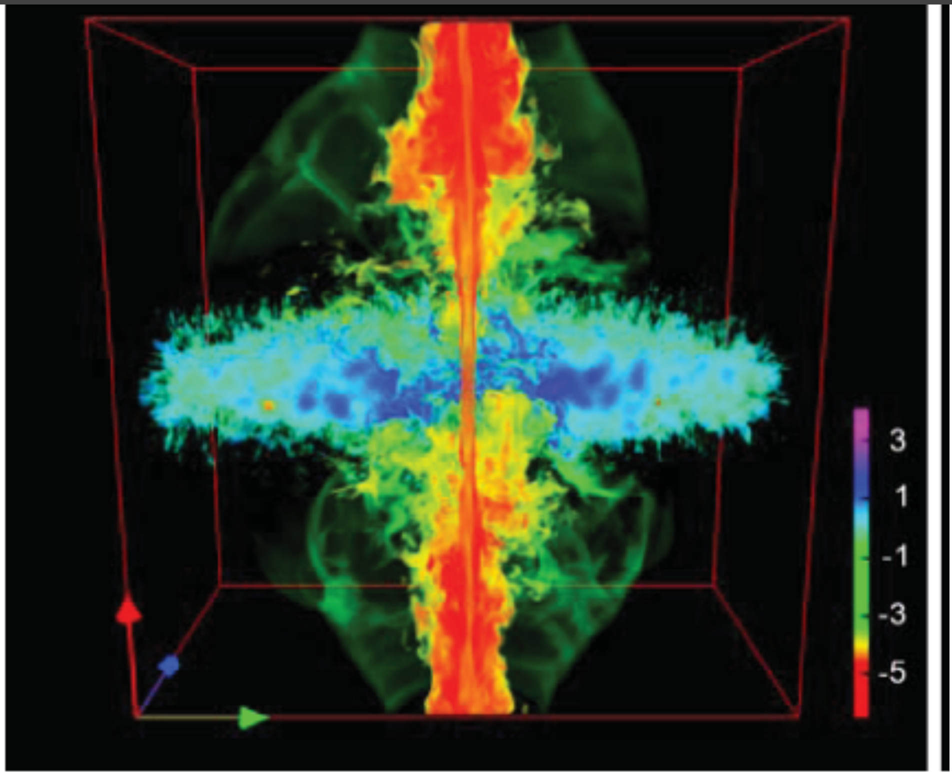

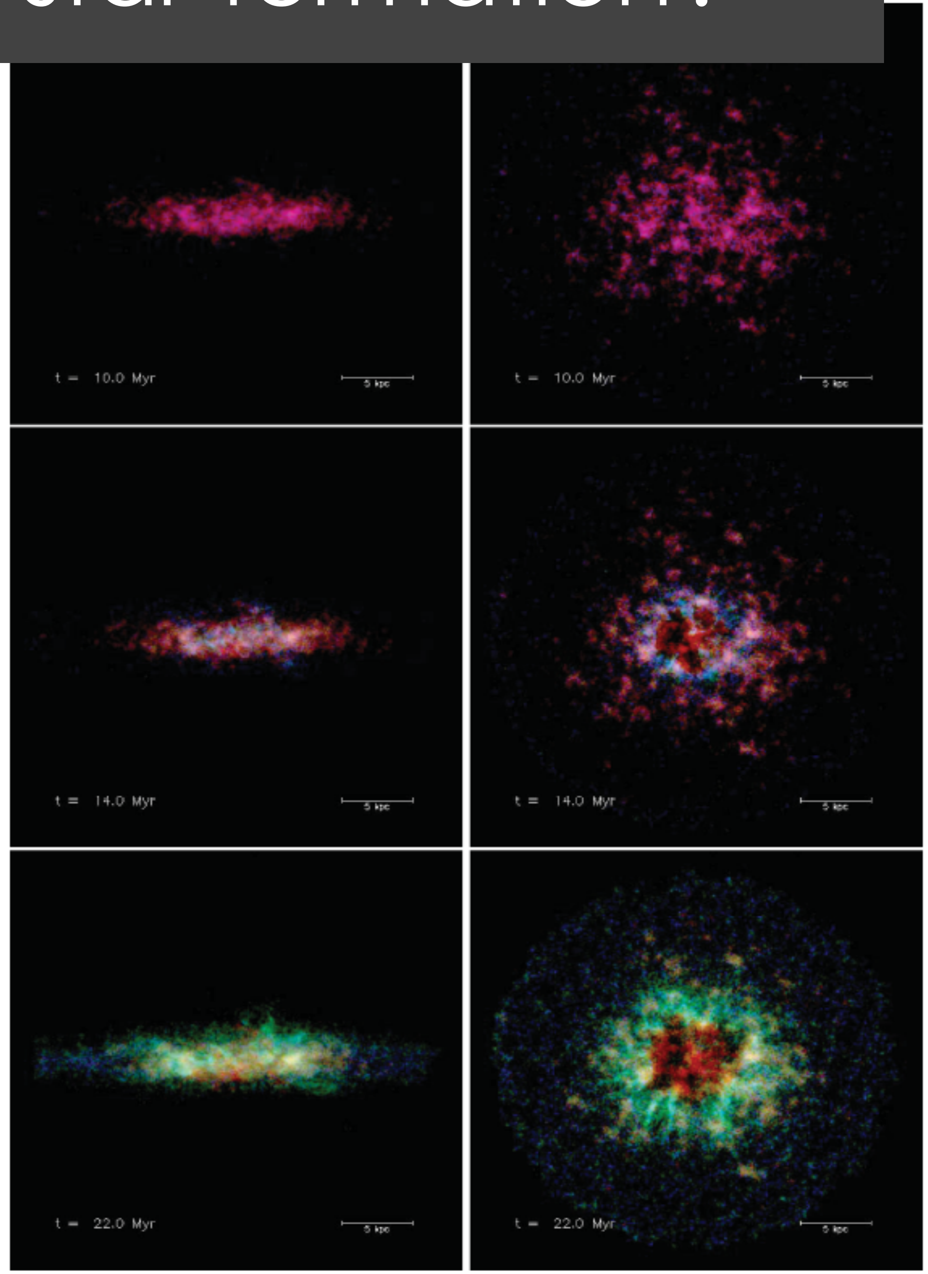

Gaibler et al. 2012:
Classical jet evolving through an inhomogeneous medium, including a massive disk of gas.
The jet triggers star formation during the first stages of evolution.

Correlation with star-formation?

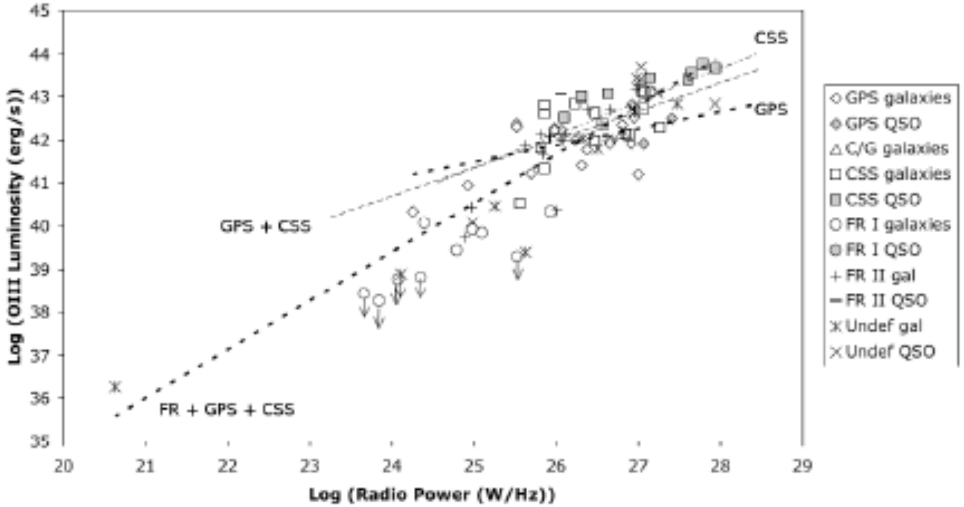

Labiano 2008

Labiano et al. 2008:

“In the CSS source 1443**+**77, the near-UV light is aligned with and is co-spatial with the radio source.”

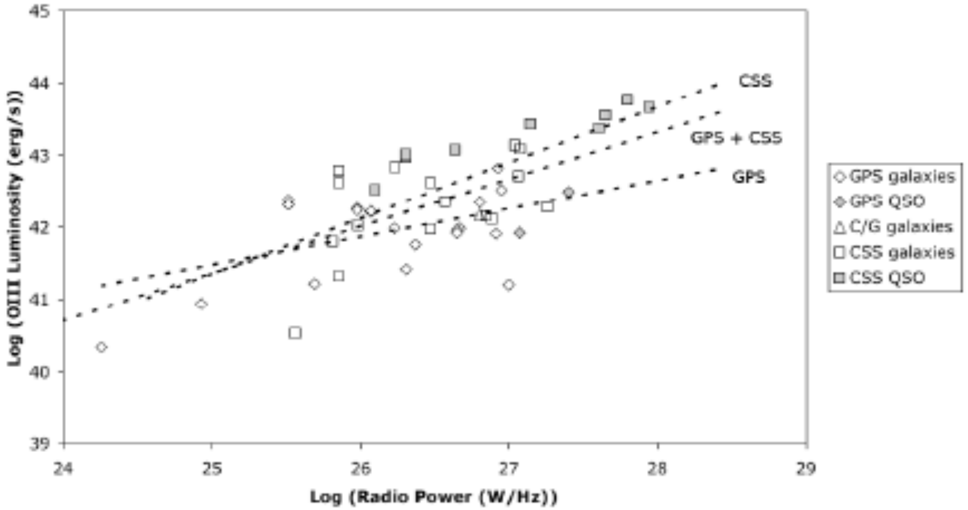

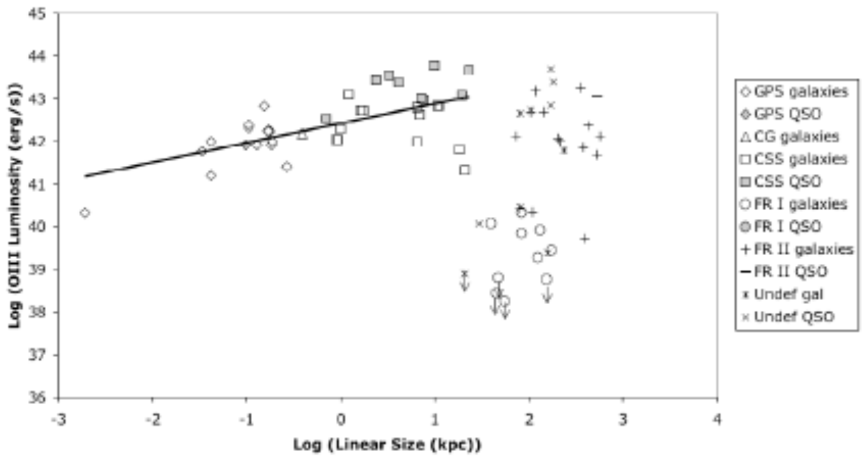

Radio-source evolution

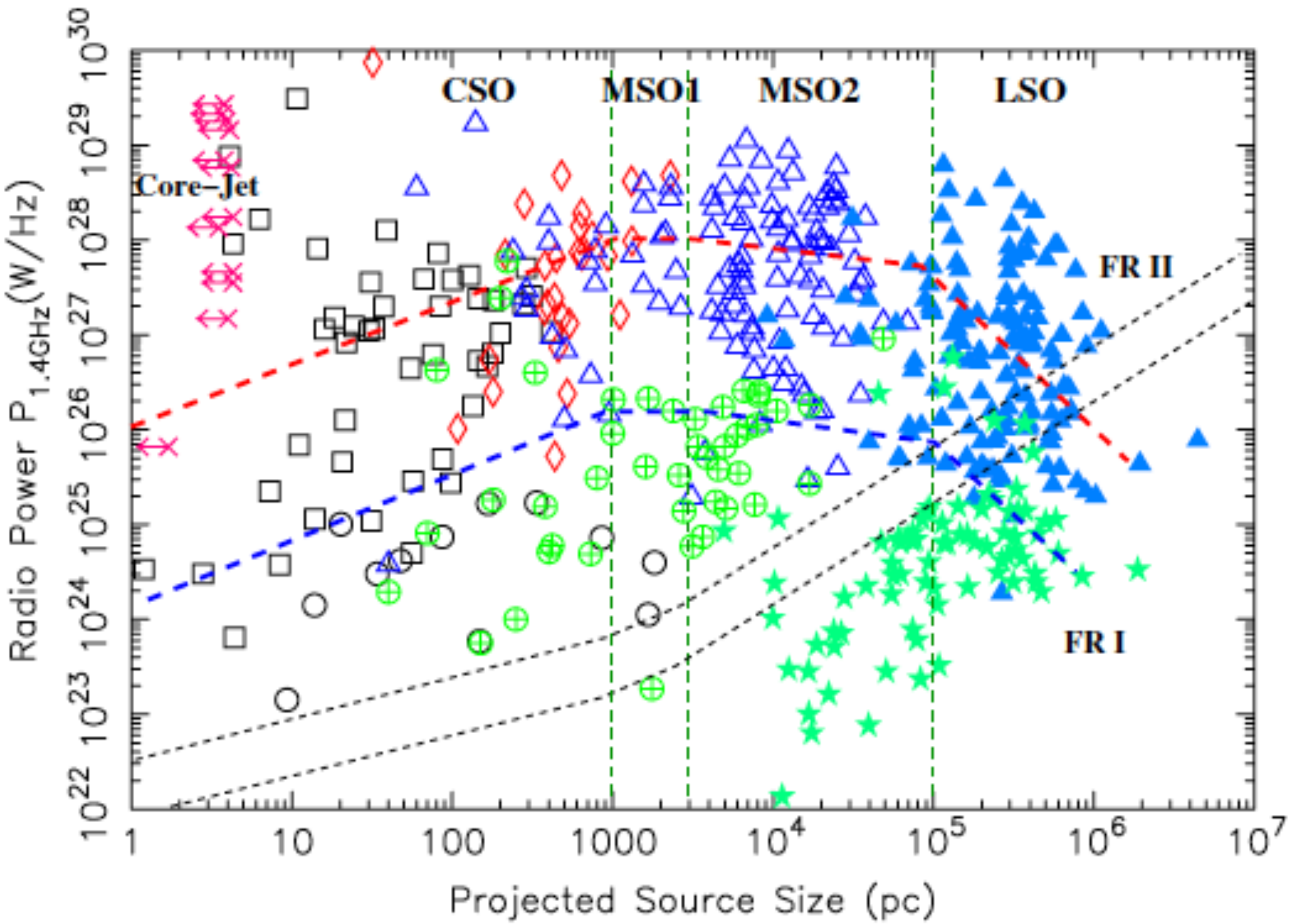

An & Baan (2012)

Deceleration mechanisms

$$n_{\rm ext}(r) = n_{\rm c}\left(1+\frac{r^2}{r_{\rm c}^2}\right)^{-3\beta_{\rm atm,c}/2} + n_{\rm g}\left(1+\frac{r^2}{r_{\rm g}^2}\right)^{-3\beta_{\rm atm,g}/2}$$

$$T = T_{\rm c} + (T_{\rm g} - T_{\rm c})\frac{r}{r_{\rm m}} \quad (r < r_{\rm m})$$
$$T = T_{\rm g} \quad (r \geqslant r_{\rm m}),$$

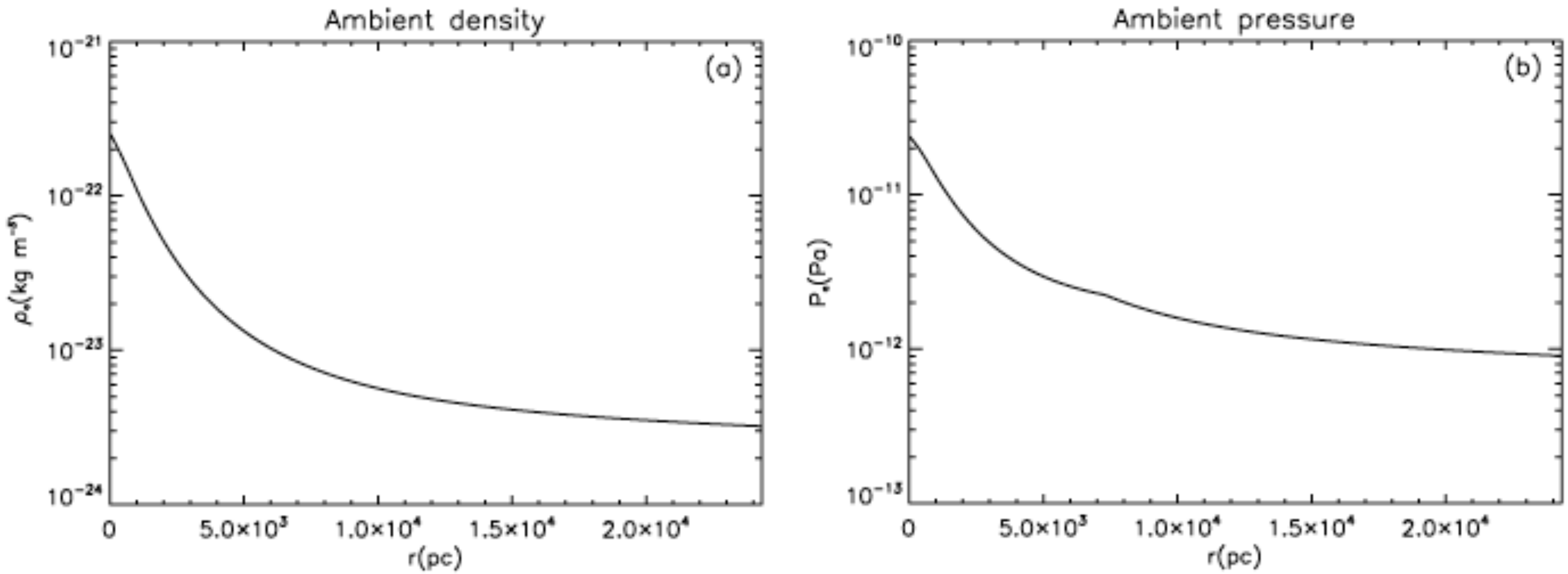

Perucho & Martí (2007)

Component	Central density	Form factor	Core radius	Temperature
Galaxy	$n_{\rm c} = 1.8 \times 10^5\,{\rm m}^{-3}$	$\beta_{\rm atm,c} = 0.73$	$r_{\rm c} = 1.2\,{\rm kpc}$	$T_{\rm c} = 4.9 \times 10^6\,{\rm K}$
Group	$n_{\rm g} = 1.9 \times 10^3\,{\rm m}^{-3}$	$\beta_{\rm atm,g} = 0.38$	$r_{\rm g} = 52\,{\rm kpc}$	$T_{\rm g} = 1.7 \times 10^7\,{\rm K}$

From Hardcastle et al. (2002)

Deceleration mechanisms

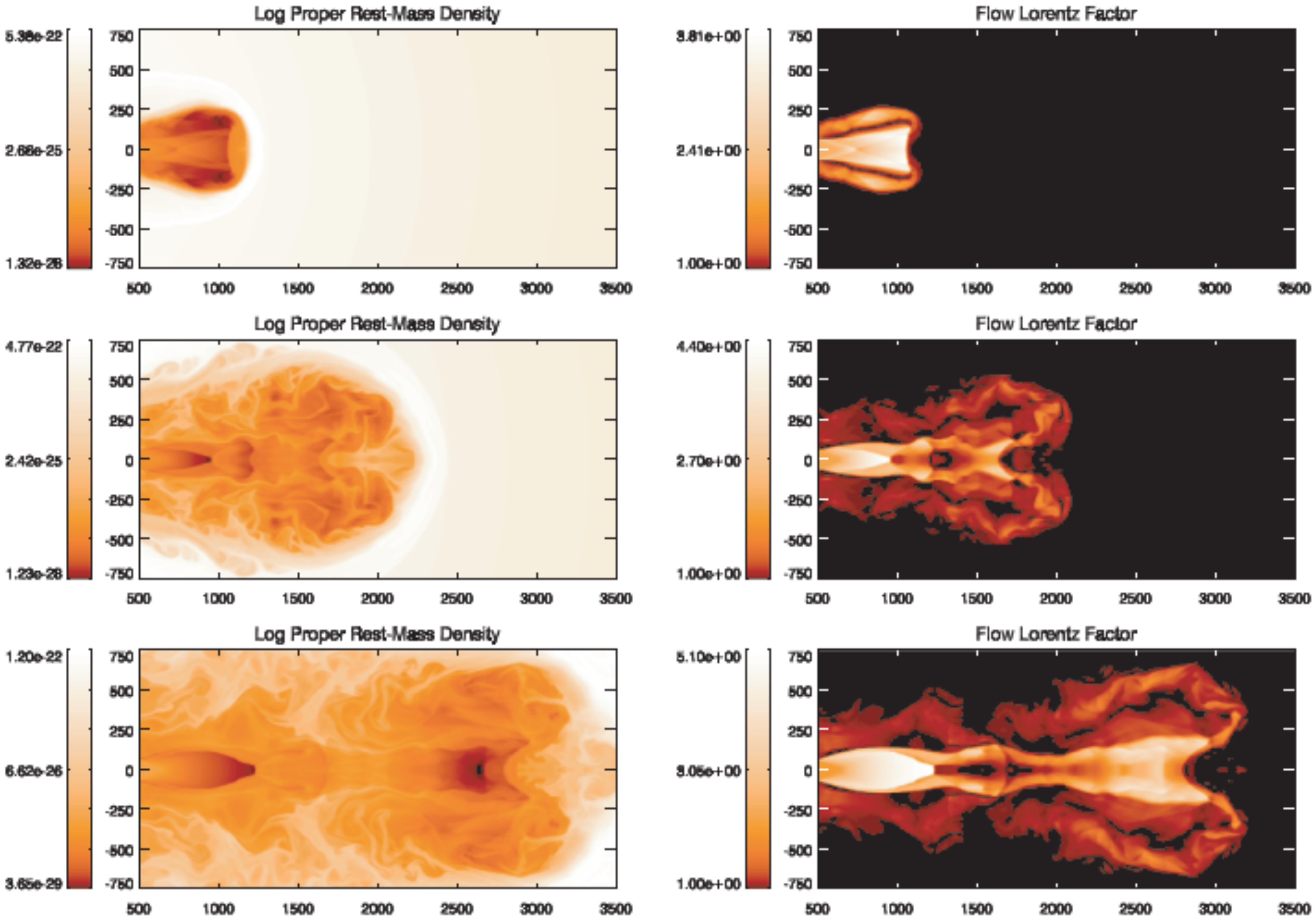

CSO

CSS

See Falle (1991), Kaiser & Alexander (1997), Maciel & Alexander (2014).

Deceleration mechanisms

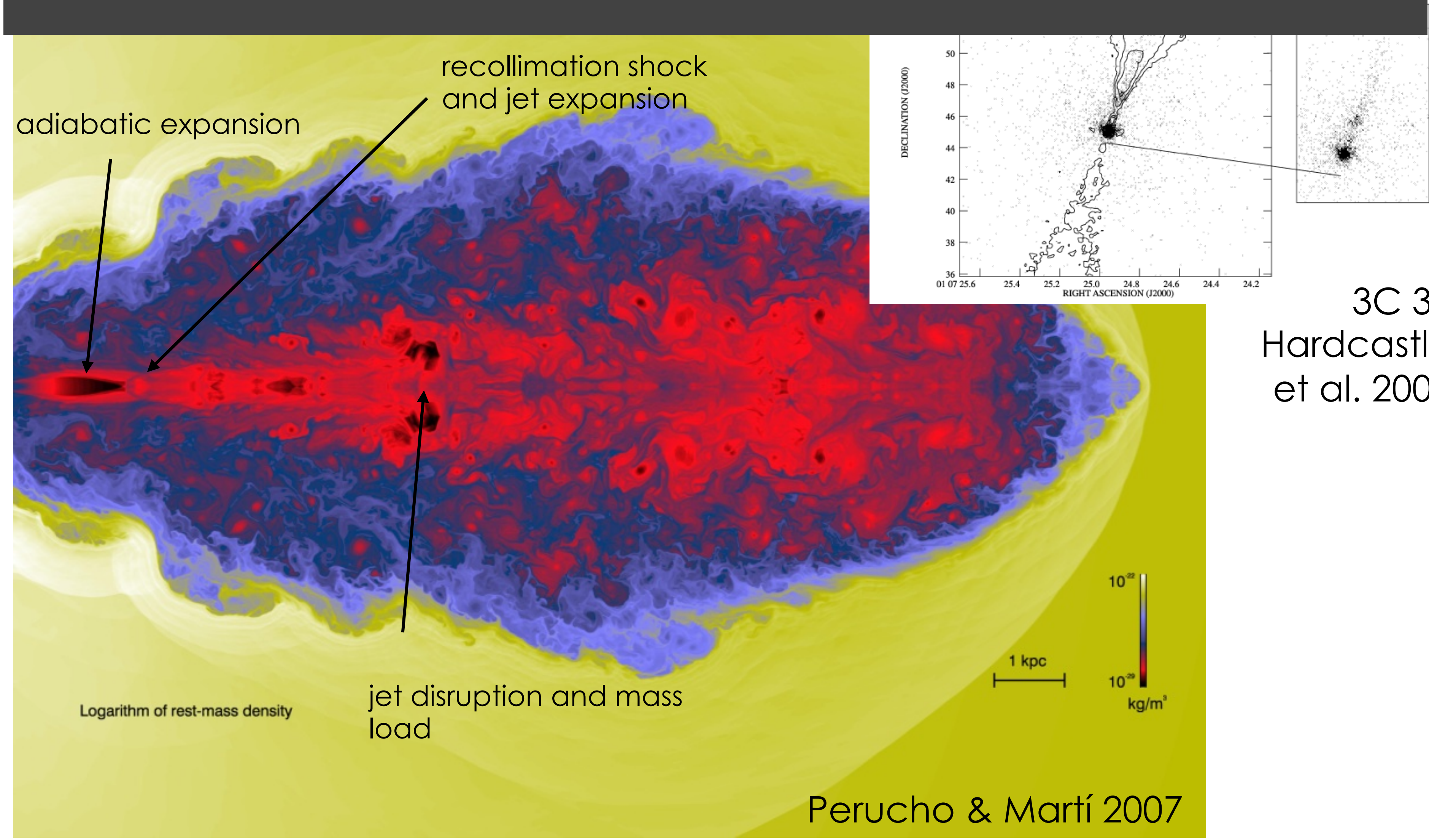

3C 31
Hardcastle
et al. 2002

Mass load and deceleration

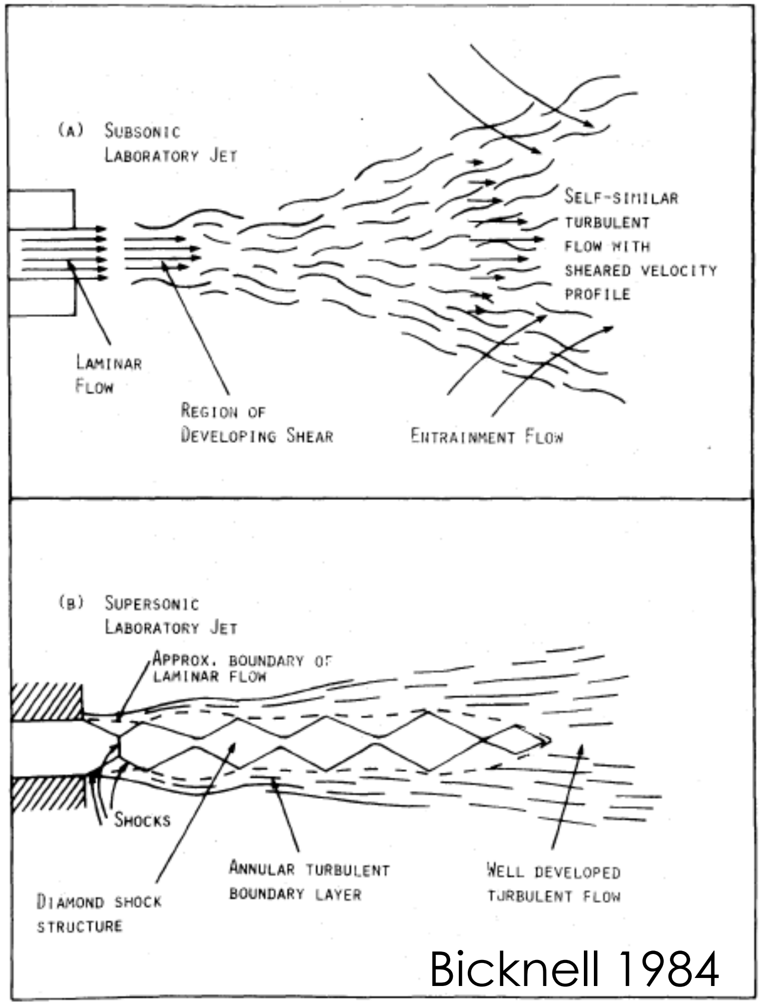

Bicknell 1984

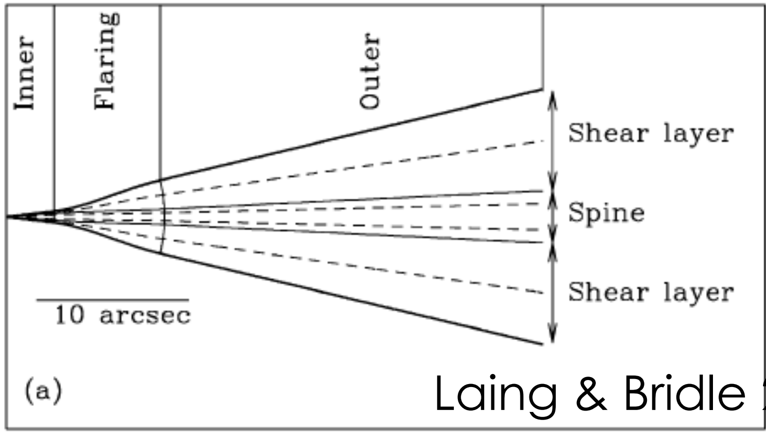

Laing & Bridle 2002

Shear-layer loading by turbulent mixing.

Wang et al. 2009

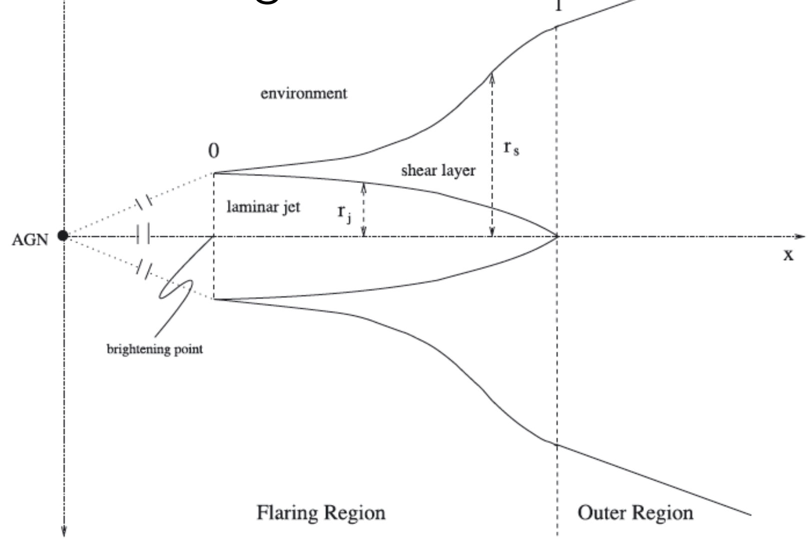

Deceleration mechanisms

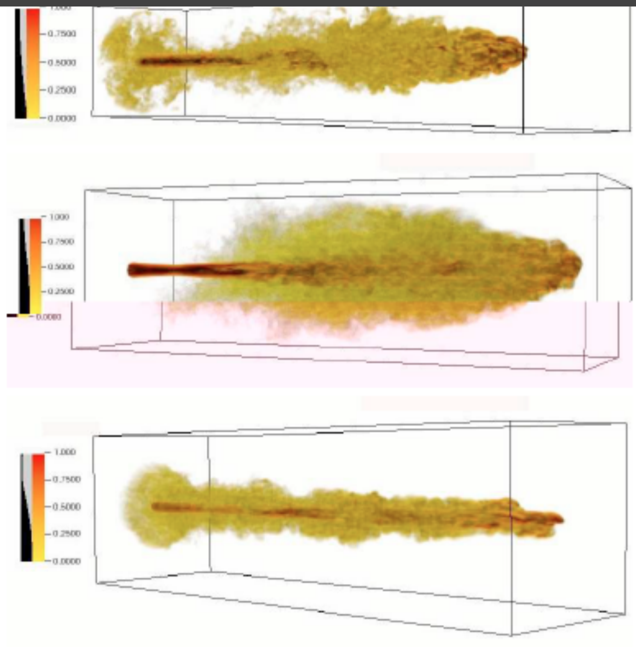

Rossi et al. 2008:
KH instability. Flaring due to the growth of long-wavelength disruptive helical modes. See Perucho, Martí-Vidal, Lobanov, Hardee (2012) for a candidate source (S5 0836+710).

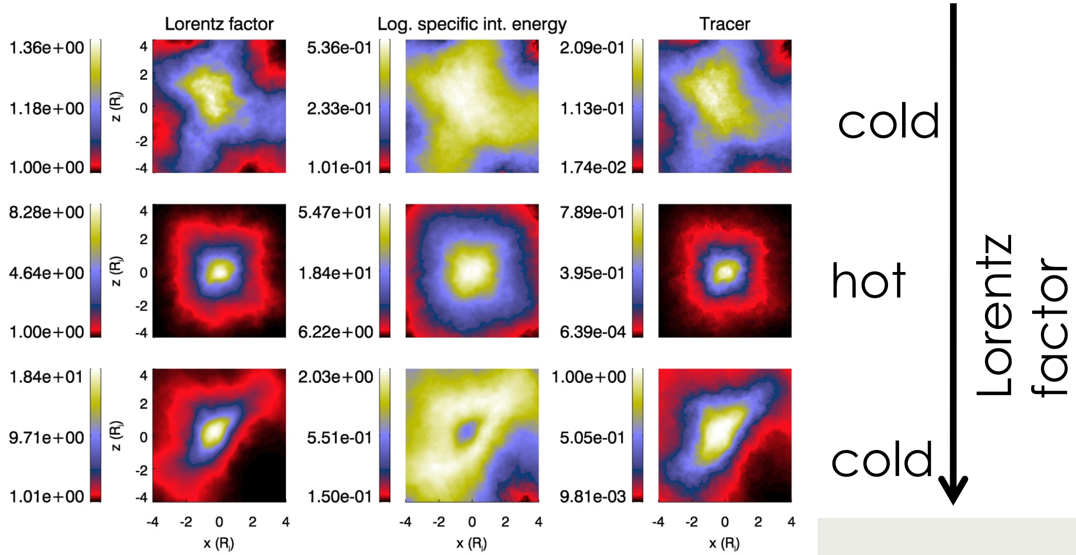

Perucho et al. 2005, 2010:
KH instability. The disruption process can be slow if the growing modes have small wavelengths.

Mass load and deceleration

Worrall et al. 2008, Goodger et al. 2010, Müller et al. 2014.
Possible interaction with obstacles in Centaurus A: Clouds, O/B type stars?

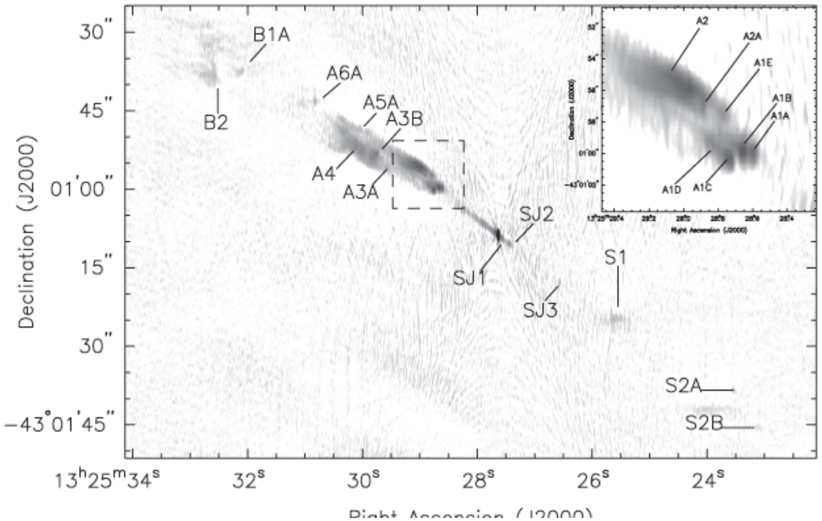

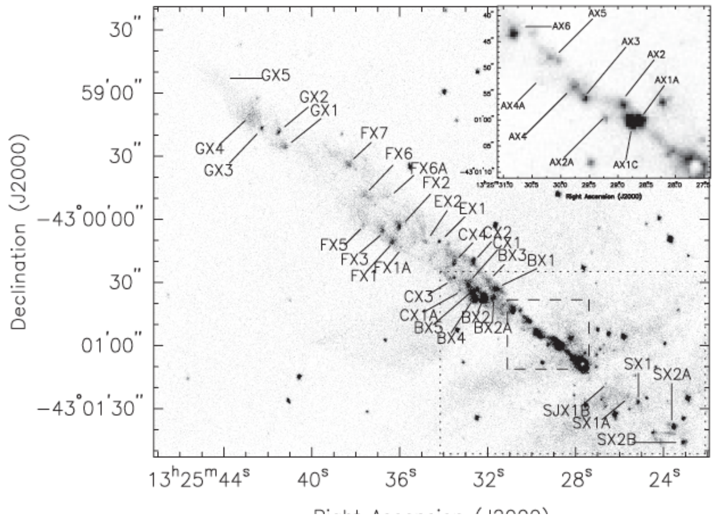

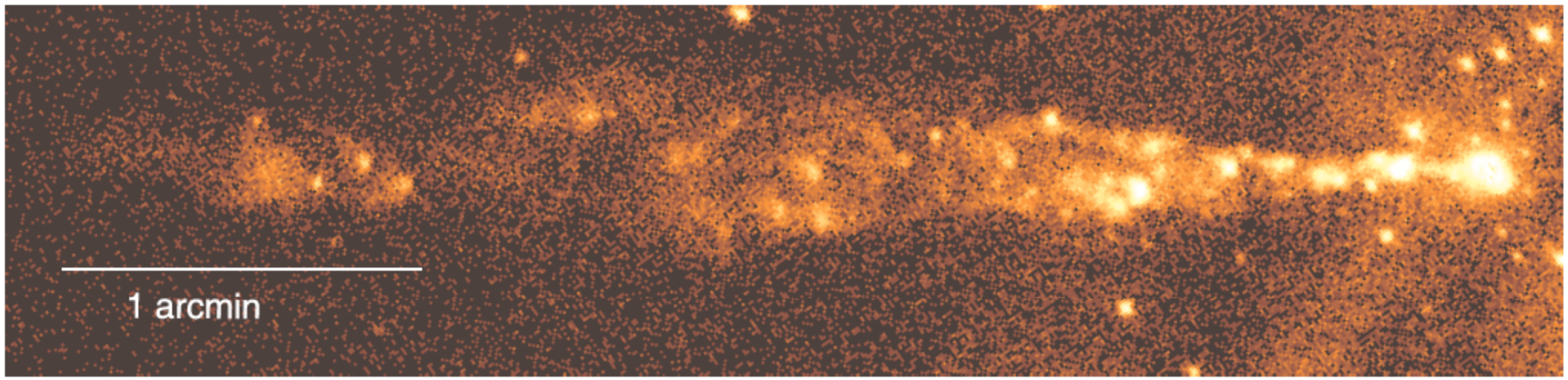

FIG. 1.—A 0.8–3 keV unsmoothed rotated image of the six *Chandra* exposures comprising the Cen A VLP, with 0.492 × 0.492 arcsec^2 pixels.

Mass load and deceleration

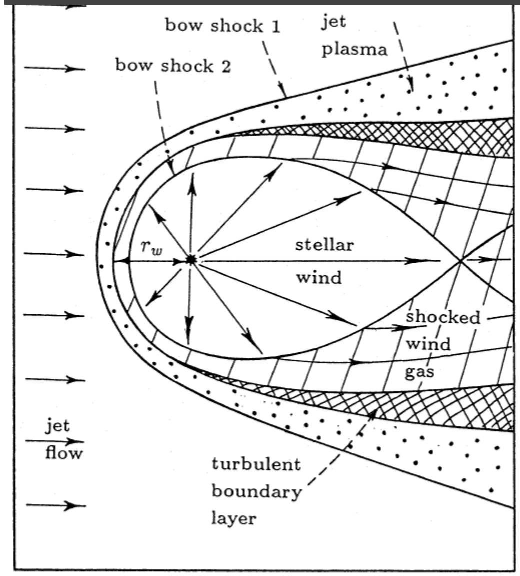

FRI deceleration due to mass-load of stellar wind gas?

Komissarov 1994 (RHD problem),
Bowman, Leahy & Komissarov 1996,
Hubbard & Blackman 2006

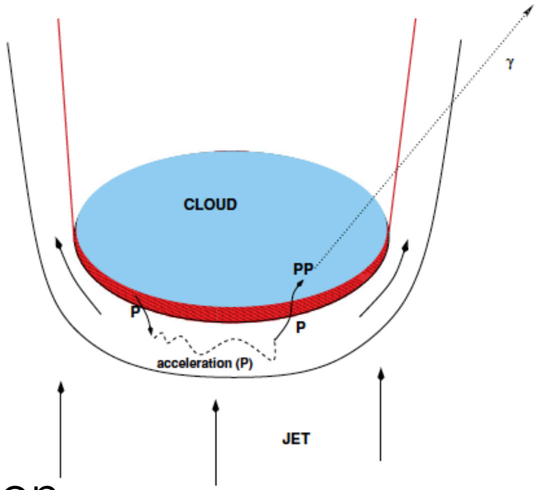

Interaction between jets and clouds invoked to explain gamma-ray emission:

Bednarek, Protheroe 1997
Araudo, et al. 2010
Barkov, et al. 2010, 2012

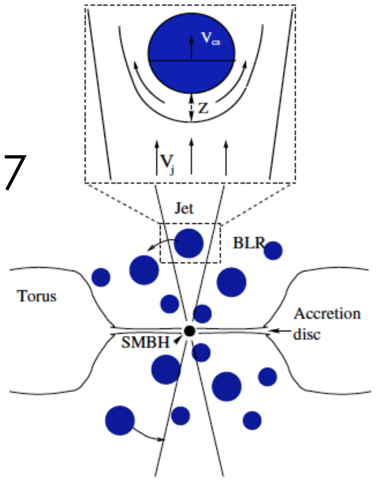

See also, e.g., Siemiginowska et al. 2008, Ostorero et al. 2010, Kino et al. 2009, Bordas et al. 2011, Kino et al. 2013, Müller et al. 2014, 2015 for discussions about the possible origin of high-energy emission in CSO's.

Mass load and deceleration

Laing & Bridle (2002) studied this case in 3C31: concluded it was not enough to decelerate the jet flow.

Following Komissarov (1994), Bowman et al. (1996), we performed simulations of FRI jets with a source term in mass accounting for mass-load from stellar wind.

Ratpenat is a high-resolution shock capturing, 3D RHD code that combines MPI and OMP parallelization. It includes **a relativistic equation of state**, taking into account different populations of particles (leptons/baryons in our case).

Model	Velocity [c]	Density [g/cm^3]	Temperature [K]	P_j/P_{am}	L_k [erg/s]	q_0 [g yr^{-1} pc^{-3}]	Jet length [kpc]	t_{sim} [Myrs]
Po	0.99	9.65×10^{-30}	3×10^9	17.6	10^{44}	4.95×10^{22}	2.2	-
Pr	0.99	9.65×10^{-30}	3×10^9	17.6	10^{44}	4.95×10^{22}	2.2	-
A0	0.95	3×10^{-33}	3×10^{11}	0.54	5×10^{41}	0	1.5	1.6
A	0.95	3×10^{-33}	3×10^{11}	0.54	5×10^{41}	4.95×10^{22}	2.1	24.0
B	0.95	3×10^{-34}	3×10^{12}	0.54	5×10^{41}	4.95×10^{22}	2.0	21.0
C	0.95	3×10^{-35}	3×10^{13}	0.54	5×10^{41}	4.95×10^{22}	1.8	19.0
D	0.95	3×10^{-35}	3×10^{13}	0.54	5×10^{41}	4.95×10^{21}	1.8	18.0

Expected evolution

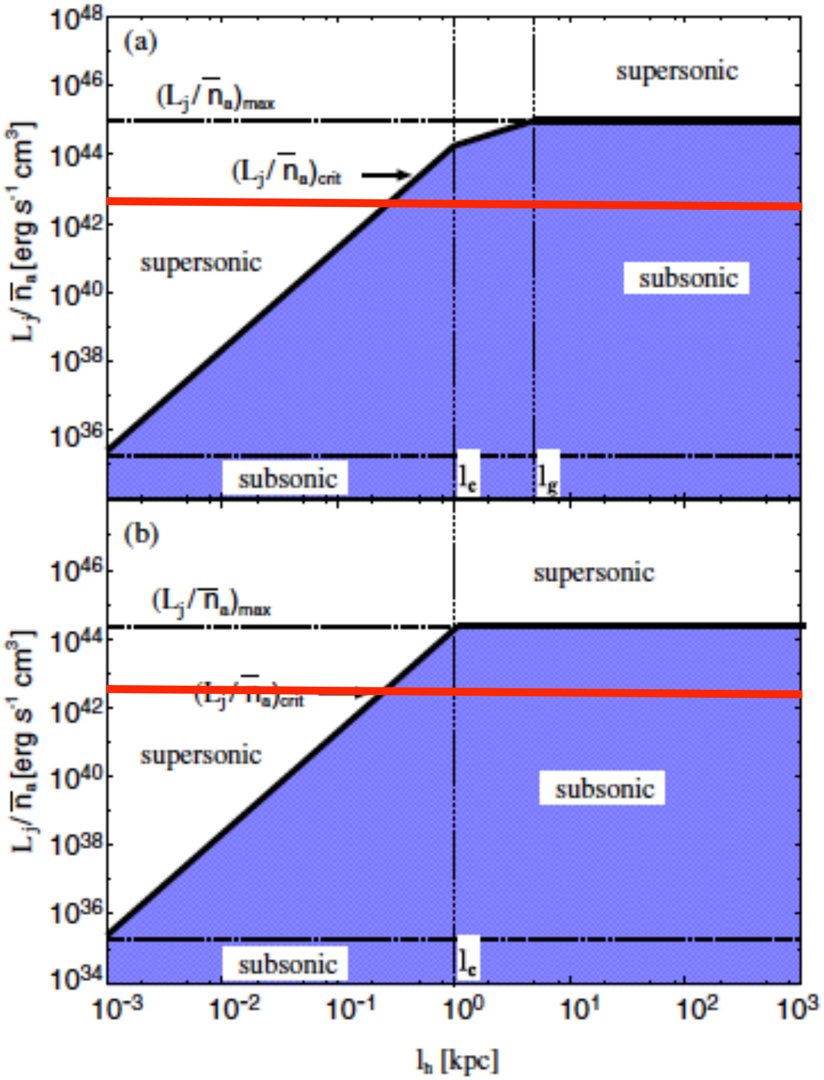

Kawakatu, Kino, Nagai (2009)

Jet power over core density (L_j/n_a) gives an estimate of the distance at which the jet will be subsonic.

The low power jets that we simulated fall on the red line.

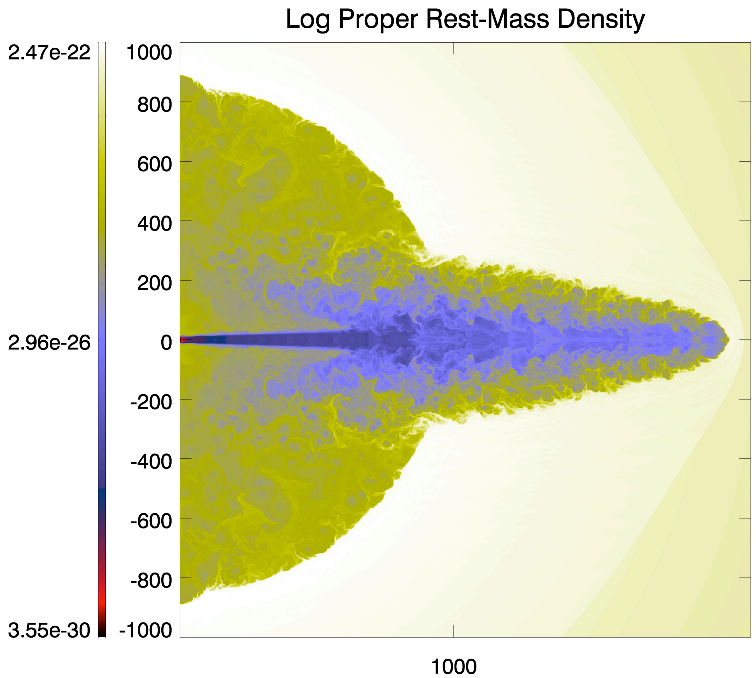

injection point at 80 pc – initial jet radius 10 pc

King density profile.

$$n_{ext} = n_c \left(1 + \frac{r^2}{r_c^2}\right)^{-3\beta_{atm,c}/2}$$

Deprojected Nuker profile (Lauer et al. 2007).

$$S_\rho = q_0 \left(\frac{r_b}{r}\right)^{\gamma} \left(1 + \left(\frac{r}{r_b}\right)^{\alpha}\right)^{(\gamma-\beta)/\alpha}$$

The stars are assumed to be all the same, with stellar mass losses 10^{-11}-10^{-12} $M_{\odot}yr^{-1}$.

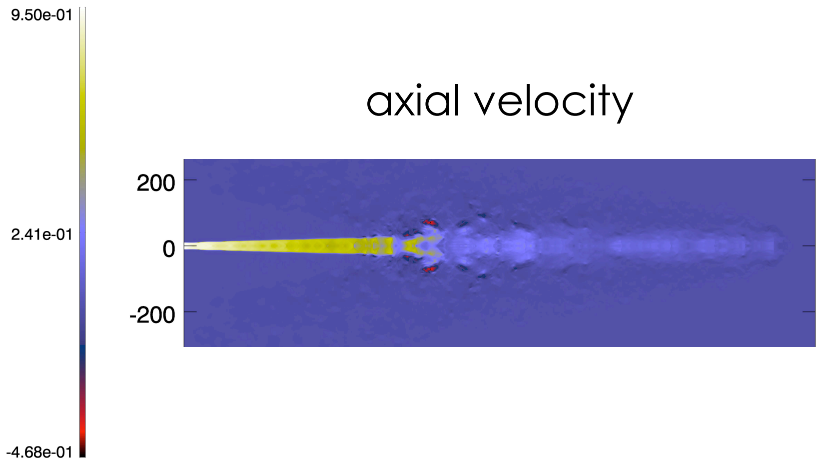

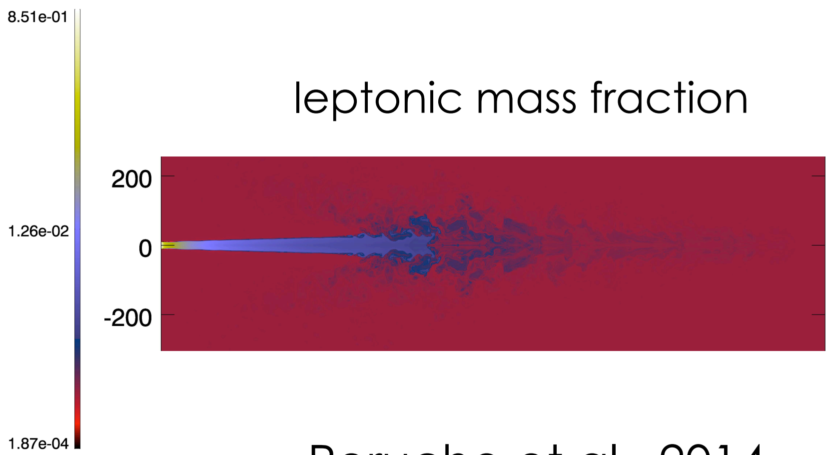

Perucho et al., 2014

Jet velocity (less or no load)

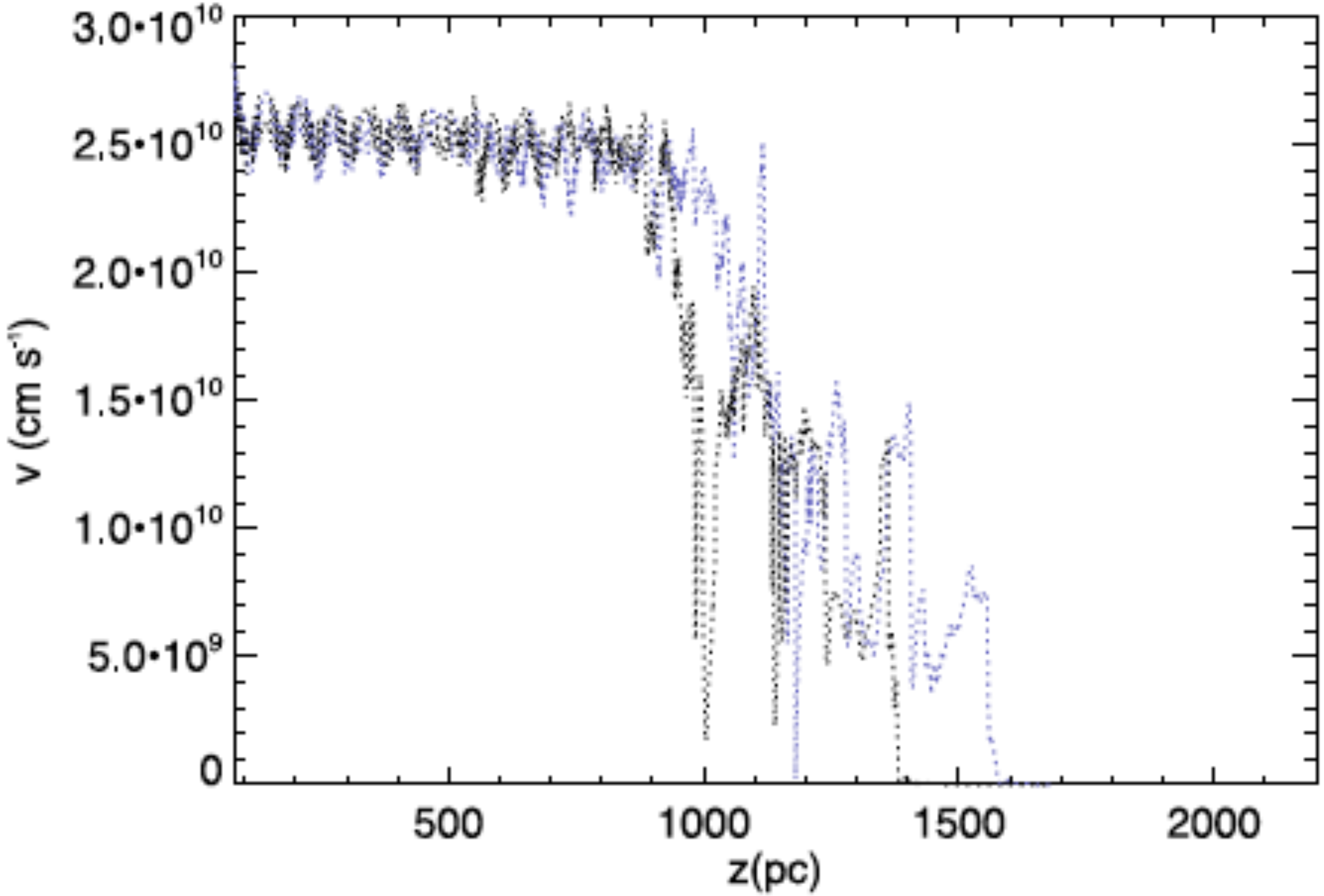

Jet velocity (mass load)

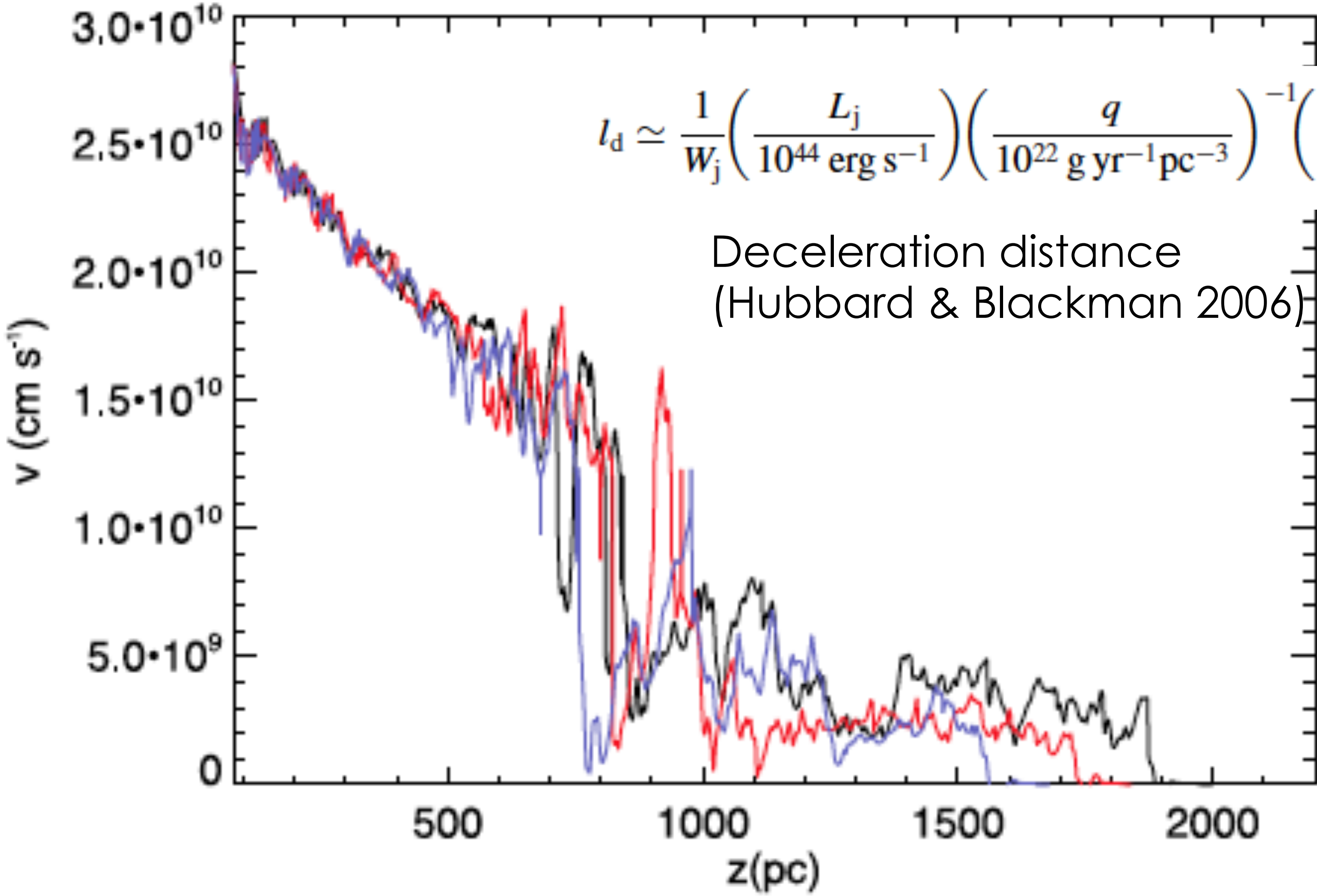

$$l_{\rm d} \simeq \frac{1}{W_{\rm j}}\left(\frac{L_{\rm j}}{10^{44}\,{\rm erg\,s^{-1}}}\right)\left(\frac{q}{10^{22}\,{\rm g\,yr^{-1}pc^{-3}}}\right)^{-1}\left(\frac{R_{\rm j}}{10\,{\rm pc}}\right)^{-2}\,{\rm Mpc}$$

Deceleration distance
(Hubbard & Blackman 2006)

Advance of the jet head

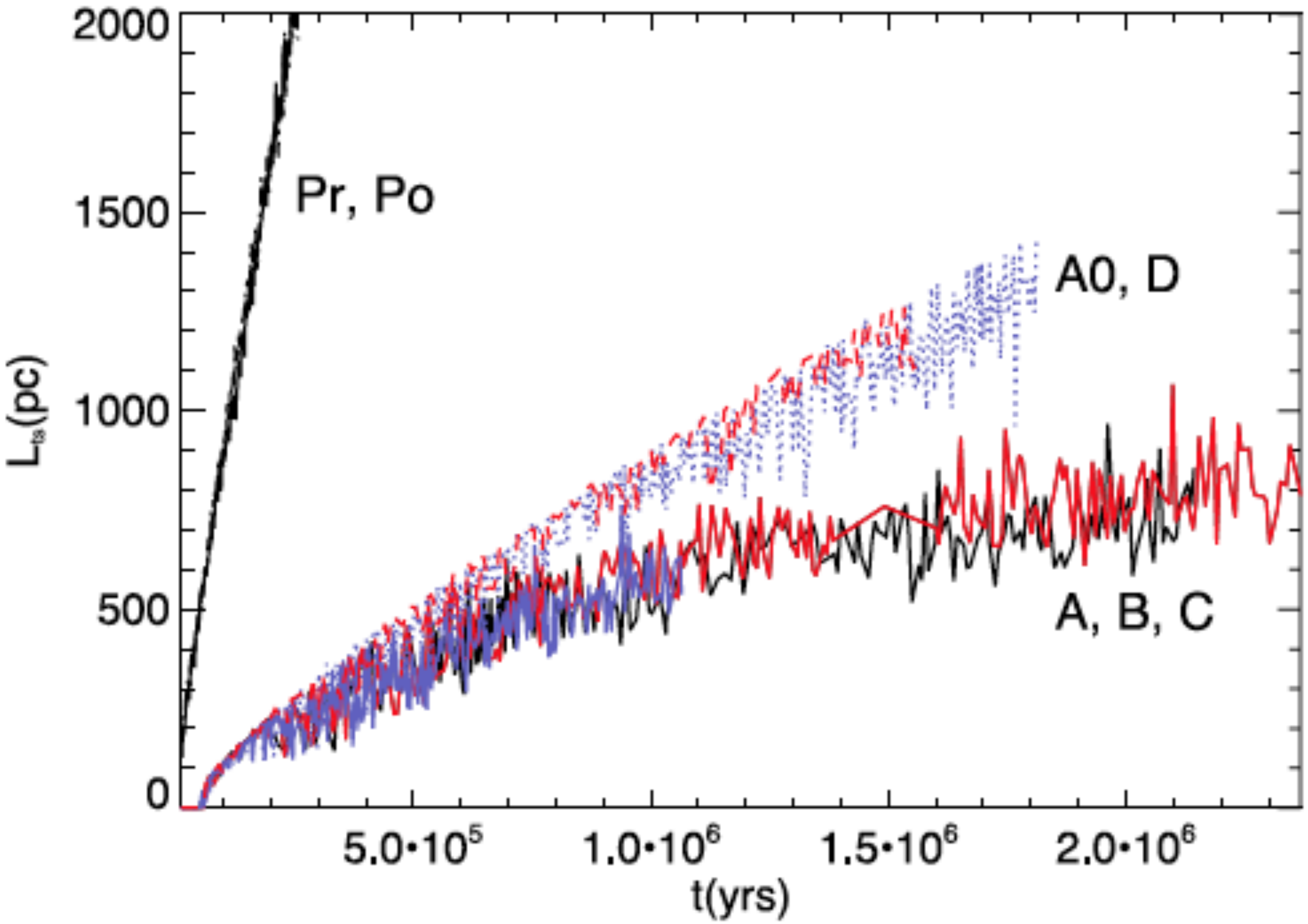

Evolution on the P-D map

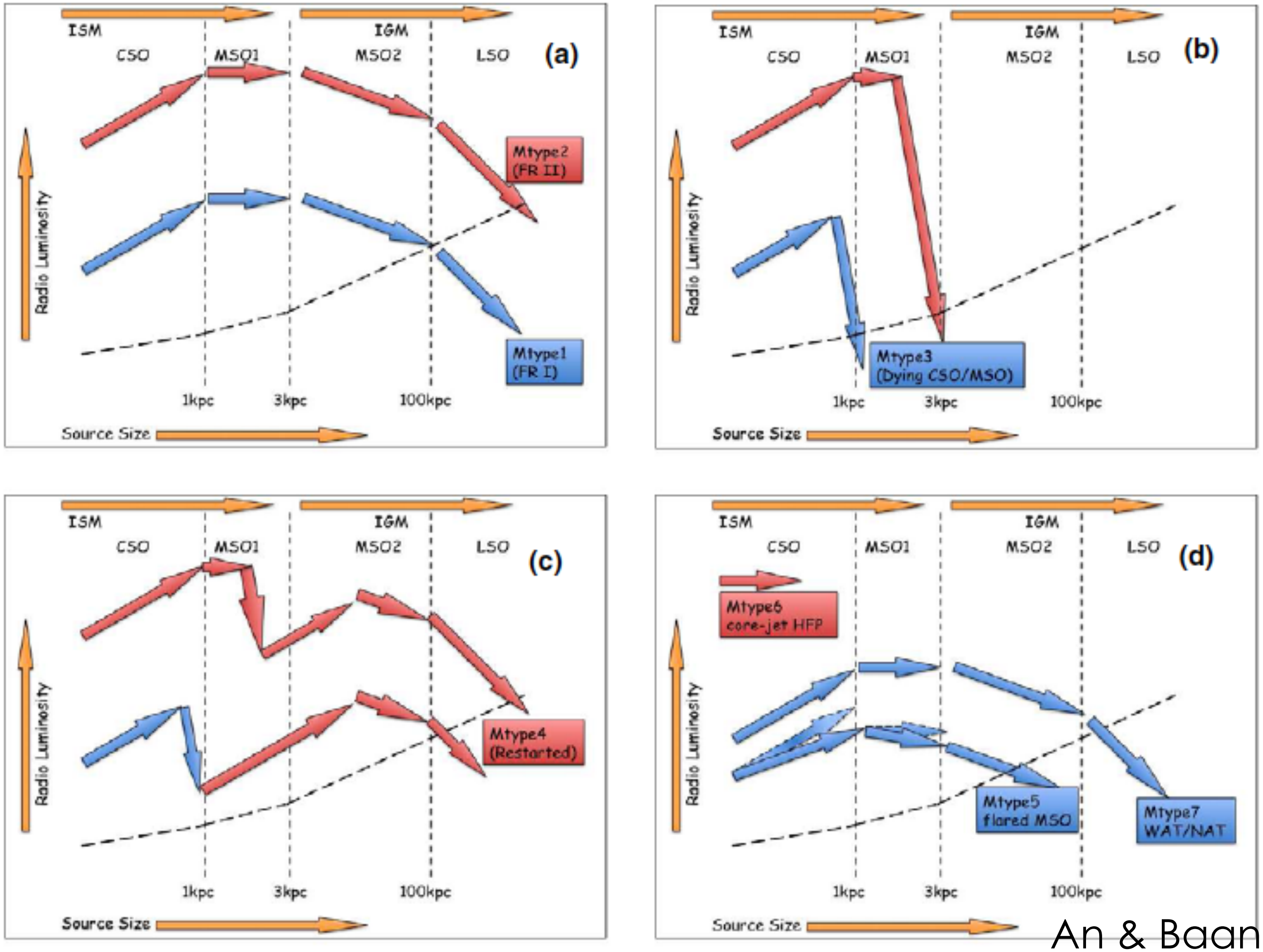

An & Baan 2012

Radio source evolution

Beyond the inner kiloparsec: Evolution of powerful radio sources

Motivation

- The gas in clusters is X-ray bright and cools.
  - Estimates of mass infall up to 100 $M_\odot$/yr (see McNamara & Nulsen 2007).

- Mechanisms invoked to stop the cooling flows:
  - Quasar mode: radiative heating.
    - Heat conduction.
    - Cosmic rays.
  - Kinetic mode: mechanical.
    - Relatively slow and massive outflows:
      - Turbulent heating in the wake of buoyant cavities.
      - Shock waves.
      - Sound waves.
    - **Relativistic jets?? (see Wagner et al. 2011/2013 for scales ≲ 1 kpc)**.

- Evidence that X-ray cavities coincide with radio-lobes (e.g., McNamara et al. 2005, Fabian et al. 2006, Nulsen et al. 2005, Fabian 2012).

2D axisymmetric hydro simulations with **Ratpenat** at the Spanish Supercomputing Network.

- Jets **injected at 1 kpc** into an atmosphere composed by neutral hydrogen with a **King-profile for density** (Hardcastle et al. 2002, Perucho & Martí 2007) in hydrostatic equilibrium.

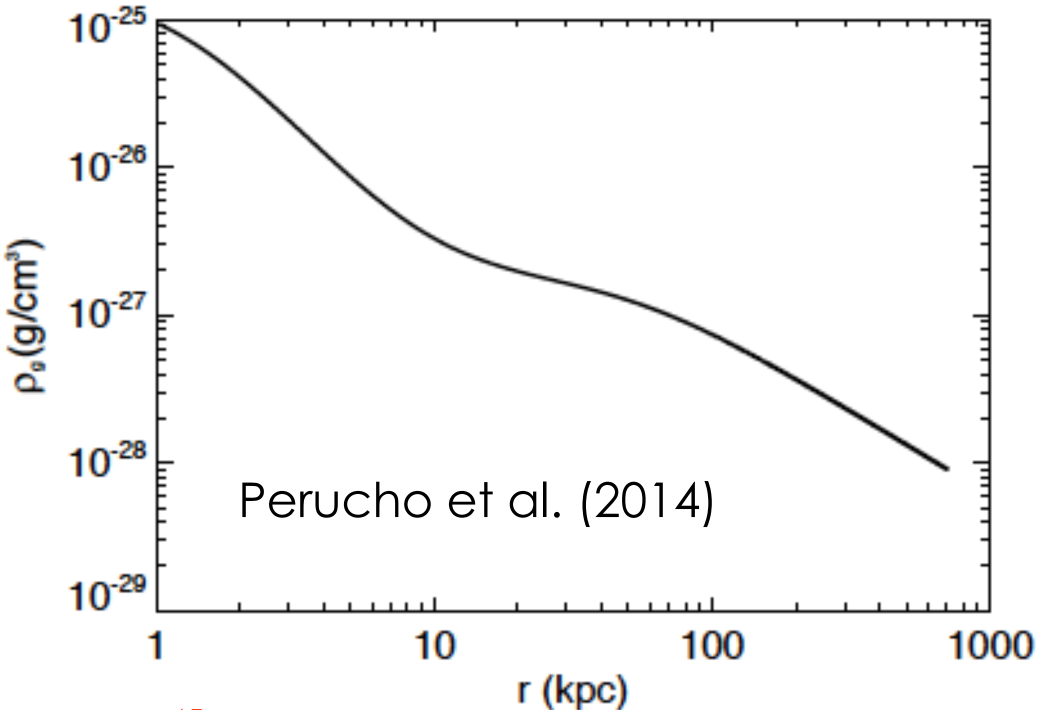

- **Jet powers**: 10^{44} erg/s (**J3** - leptonic) – 10^{45} erg/s (**J1** –leptonic, **J4** - baryonic) – 10^{46} erg/s (**J2** - leptonic).
    - Jet radius: 100 pc. Jet velocity: 0.9 – 0.99 c

- Injected during **16 to 50 Myr**. The simulations last for 200 Myr.

- Resolution: 50x50 pc or 100x100 pc per cell in the central region (Total 16000x2000 cells, **800 /900 kpc x 500 kpc**).

- Time steps of 50-100 years during the first stages of evolution.

Expected evolution

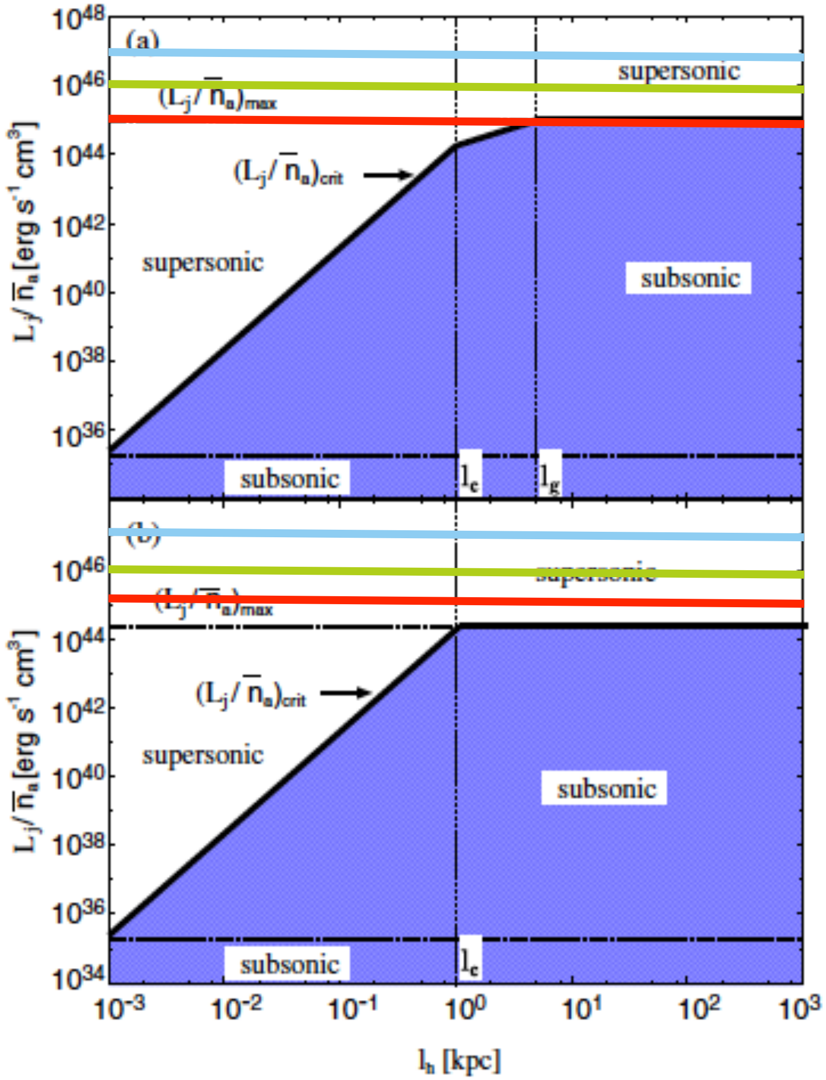

Kawakatu, Kino, Nagai (2009)

Jet power over core density (L_j/n_a) gives an estimate of the distance at which the jet will be subsonic.

The high-power jets fall on the colour lines.

Bow-shock advance speed vs time

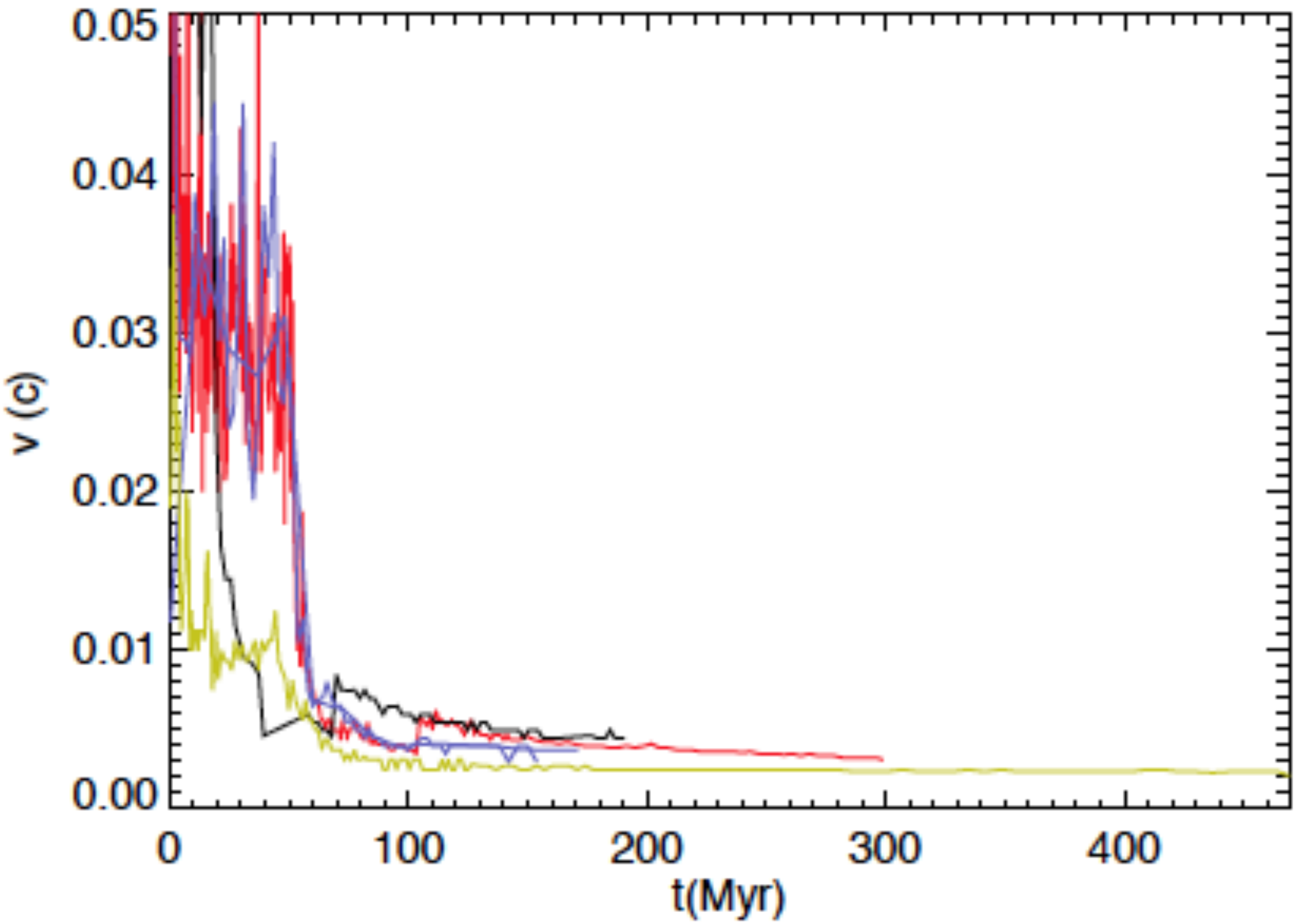

Bow-shock position vs time

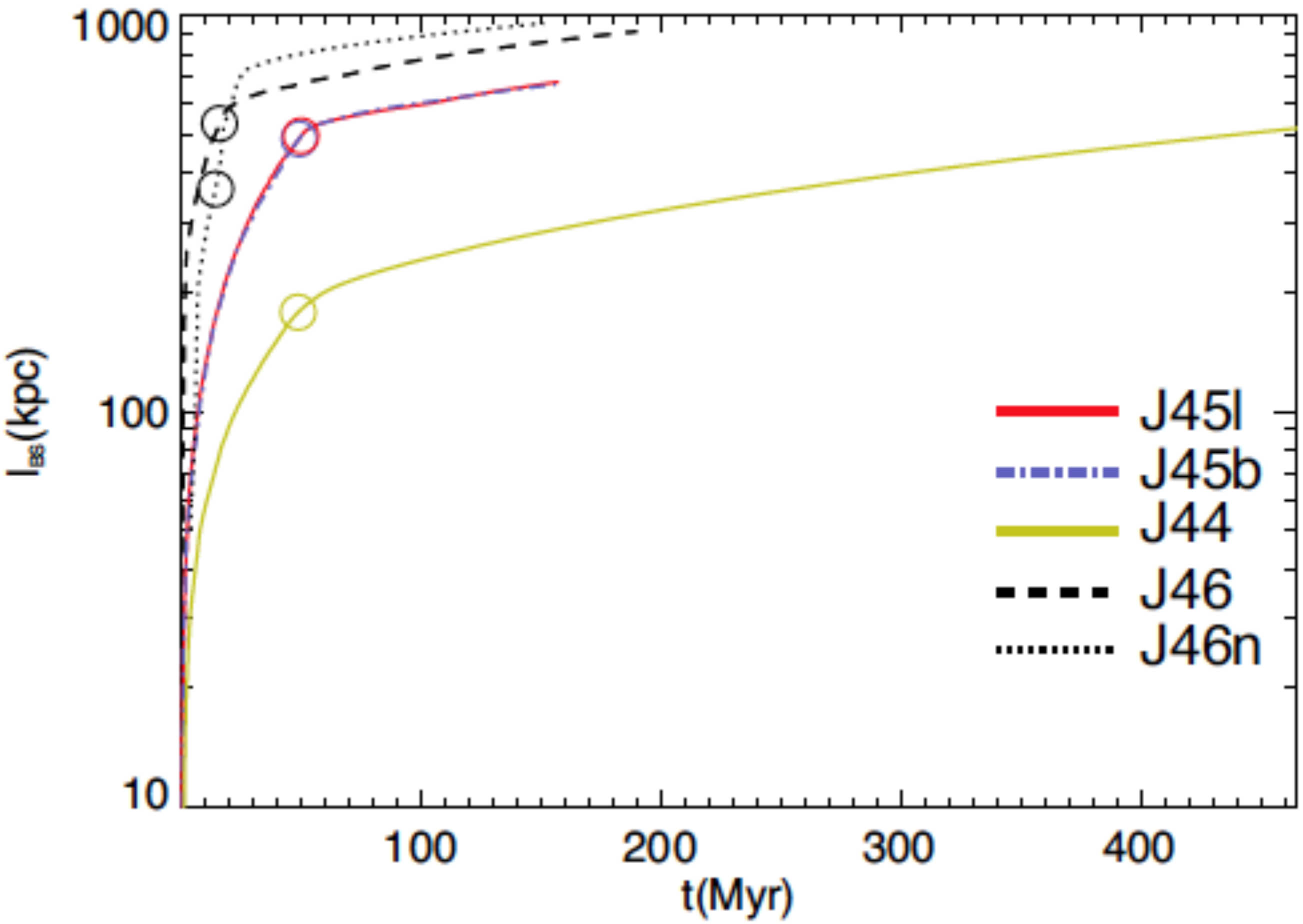

Bow-shock Mach number vs time

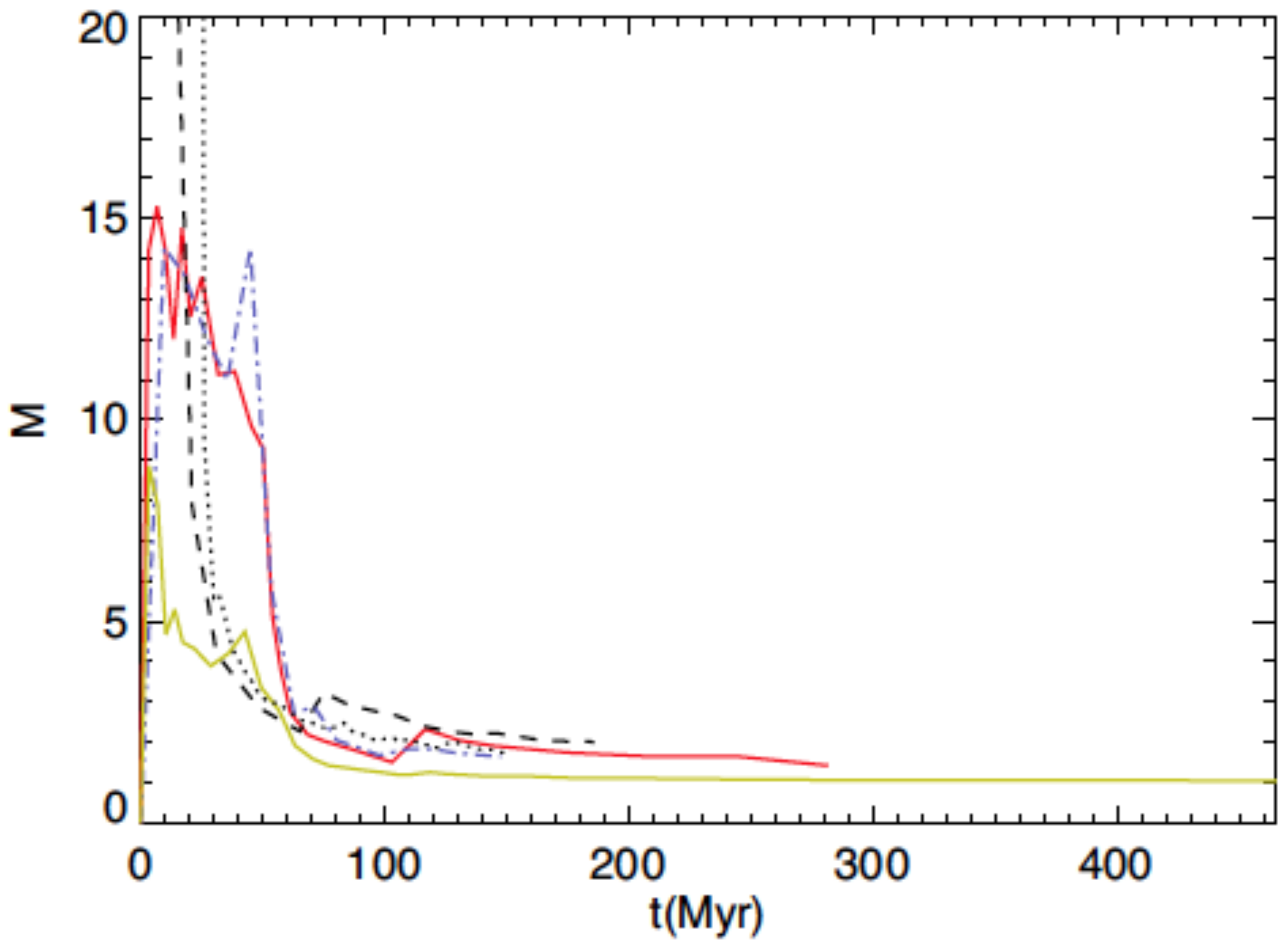

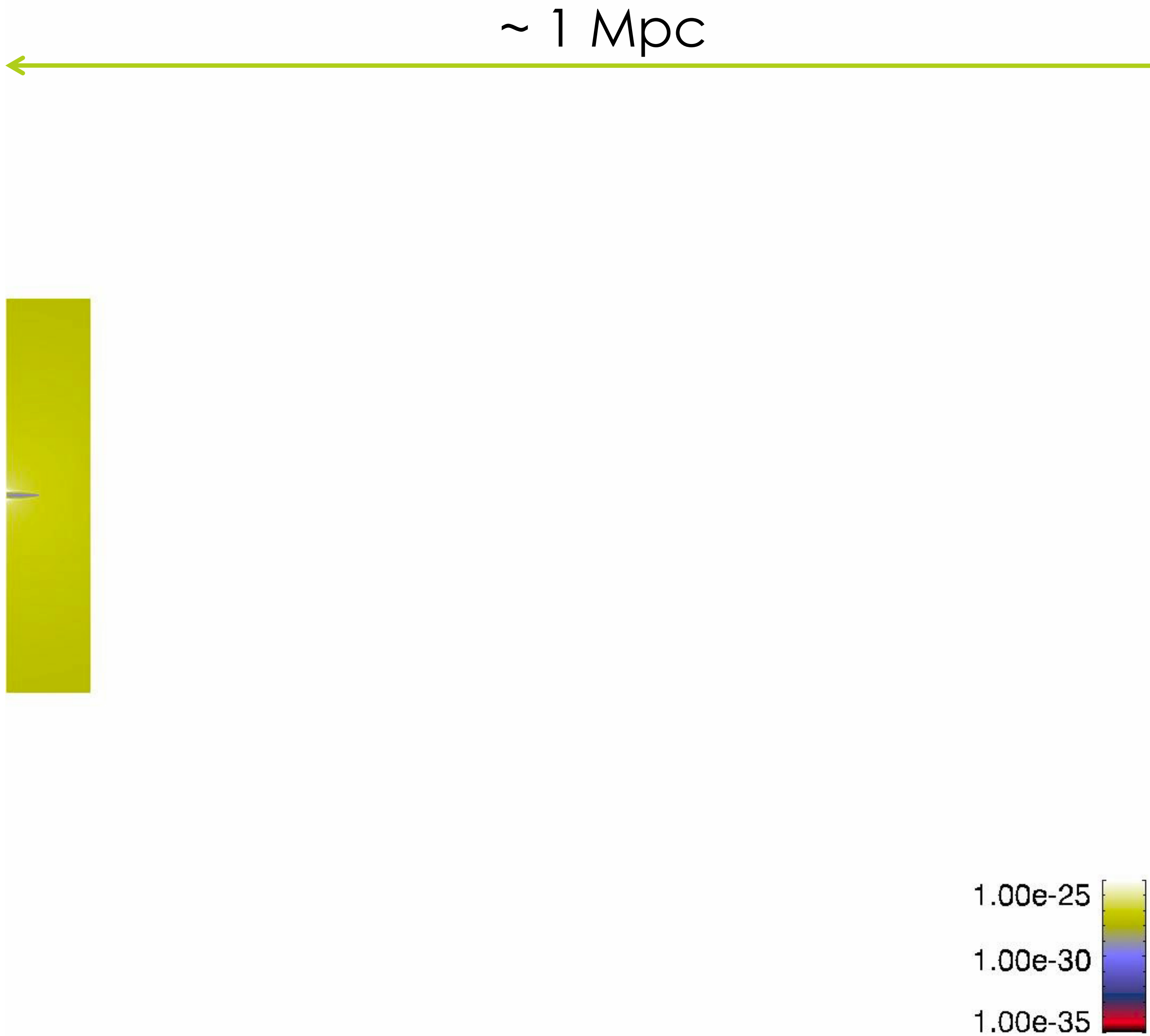
~ 1 Mpc
1.00e-25
1.00e-30
1.00e-35

J2

10 Myr

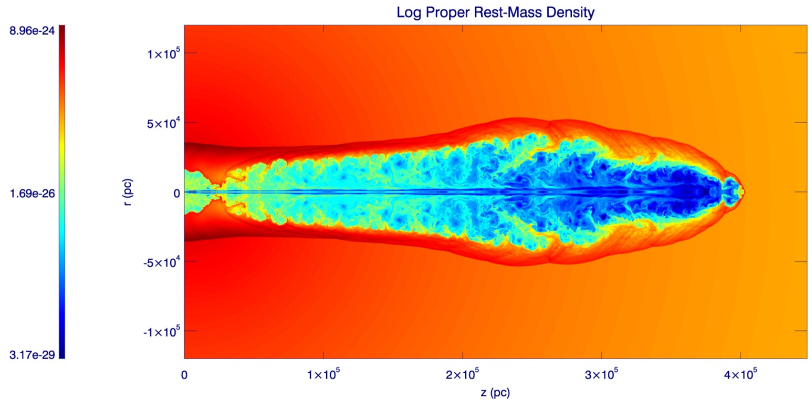

Log Proper Rest-Mass Density
8.96e-24
1.69e-26
3.17e-29
1×10^5
5×10^4
0
-5×10^4
-1×10^5
r (pc)
0
1×10^5
2×10^5
3×10^5
4×10^5
z (pc)

J2

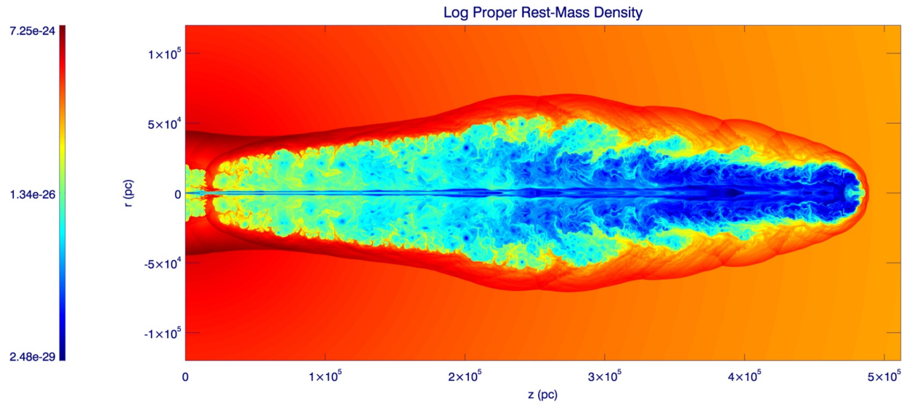

15 Myr

J2

30 Myr

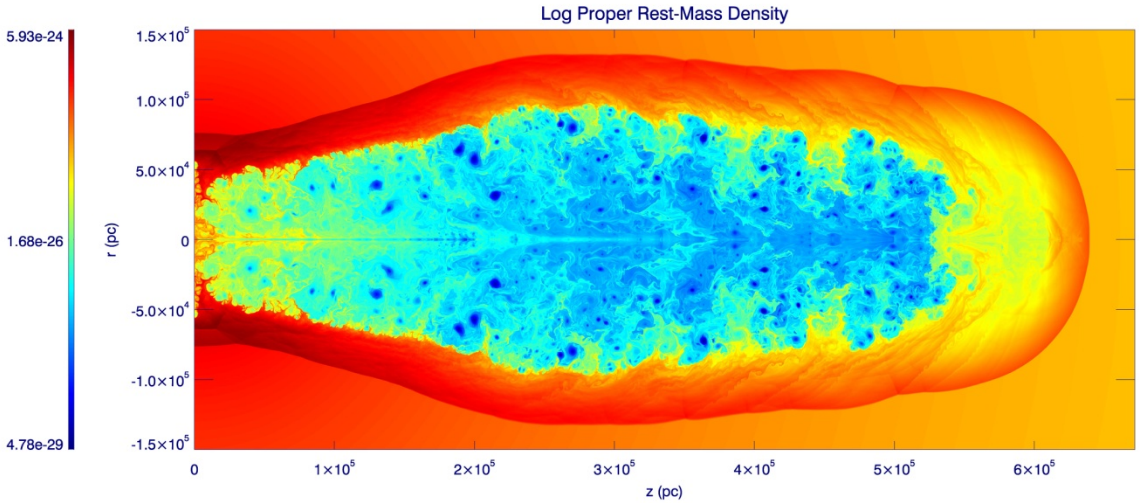

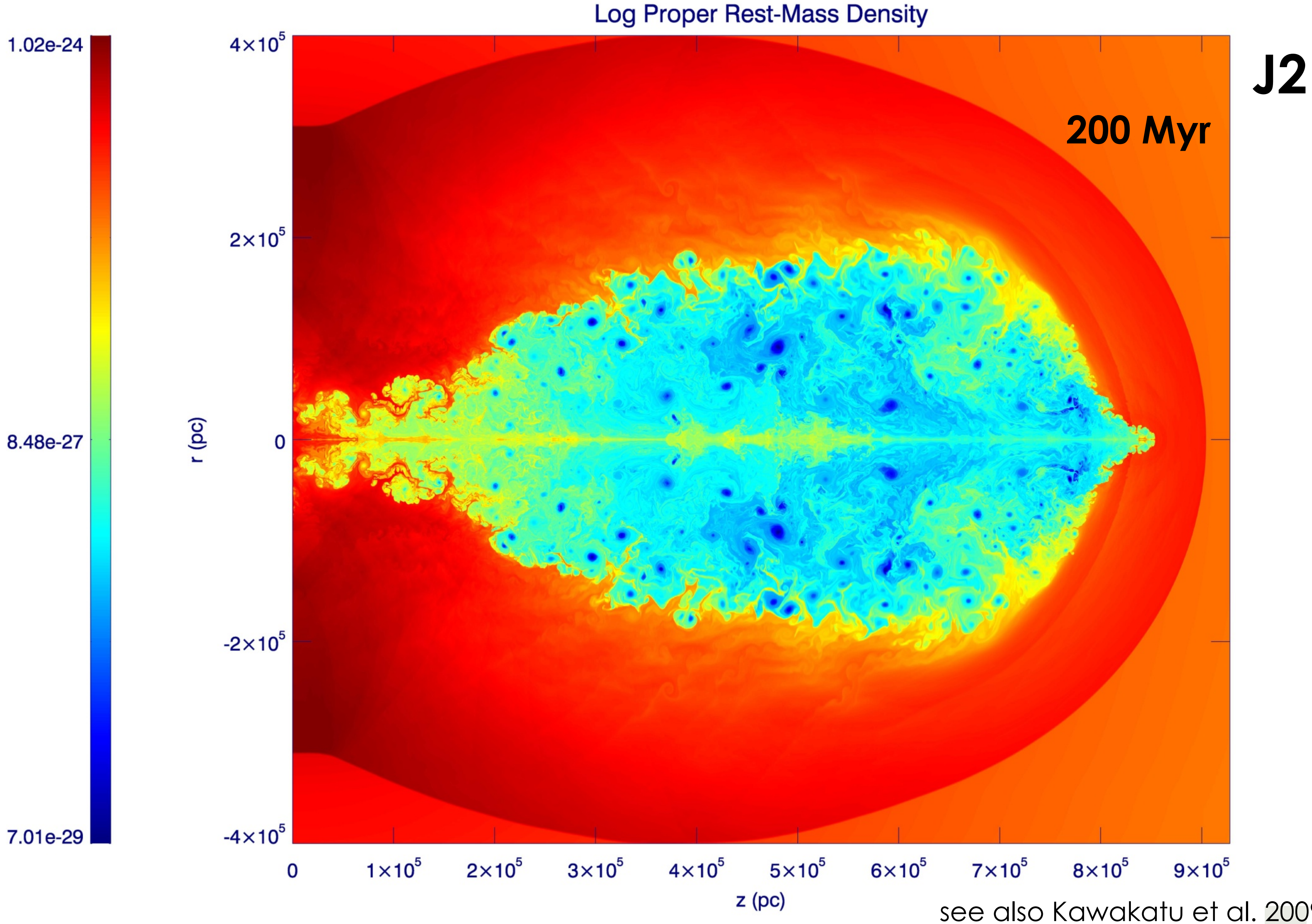

see also Kawakatu et al. 2009

Final picture

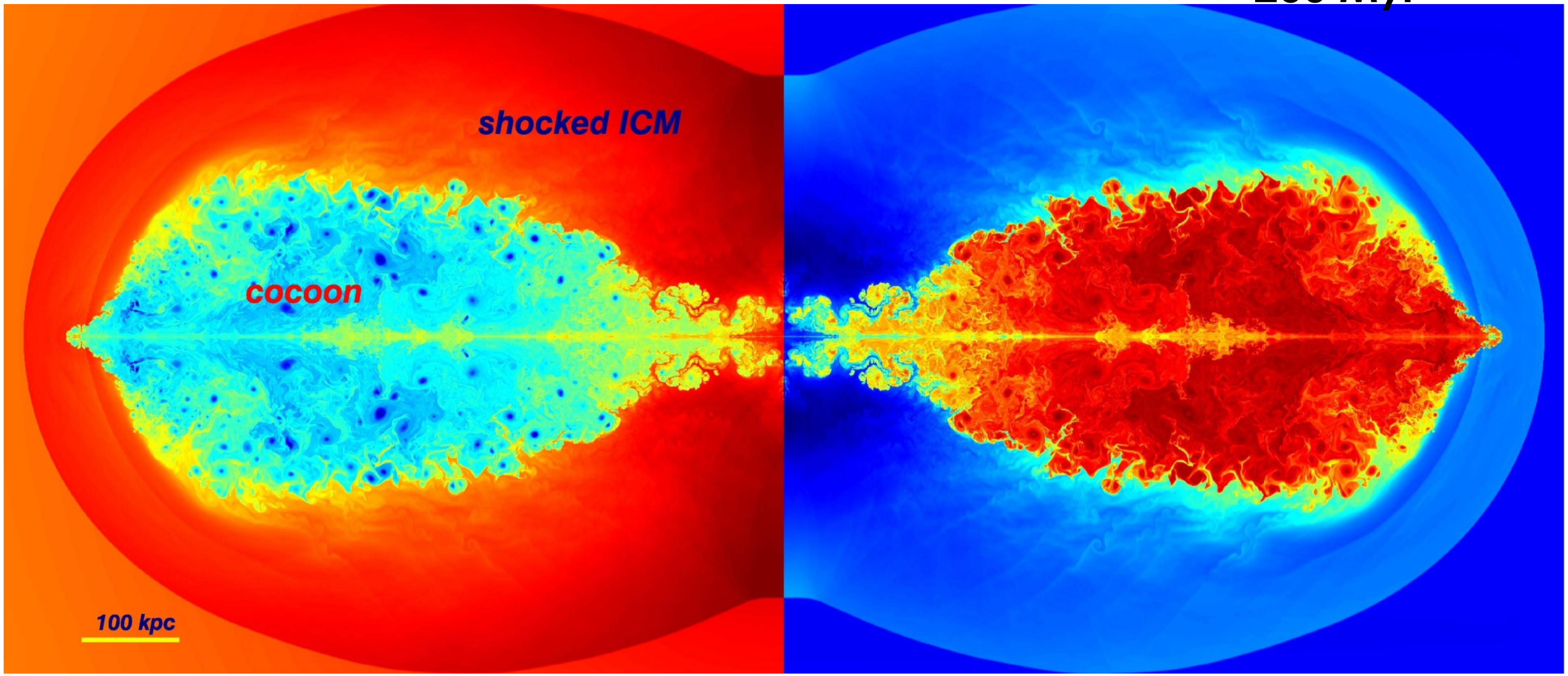

Perucho et al. 2011, ApJ

10^{46} erg/s

Efficiency

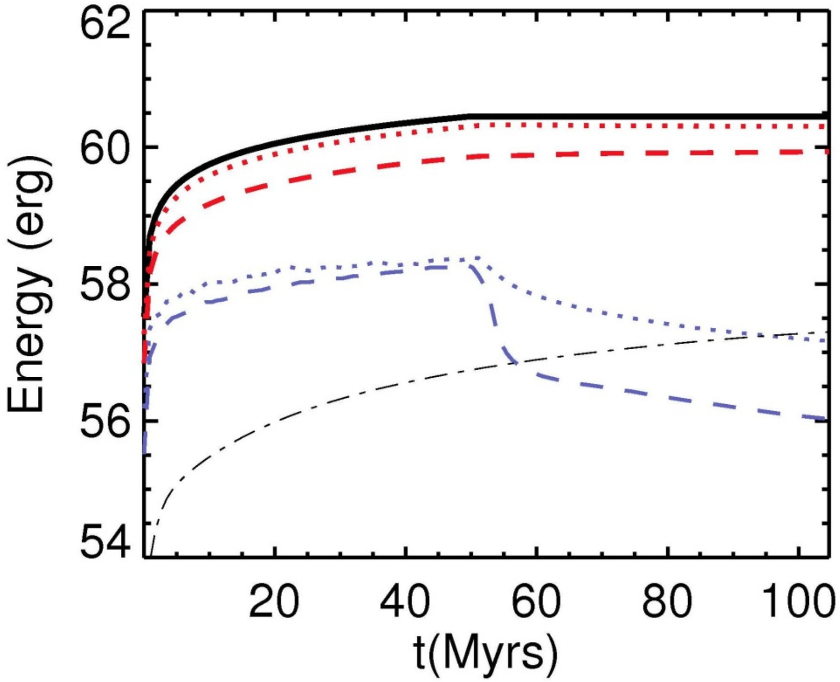

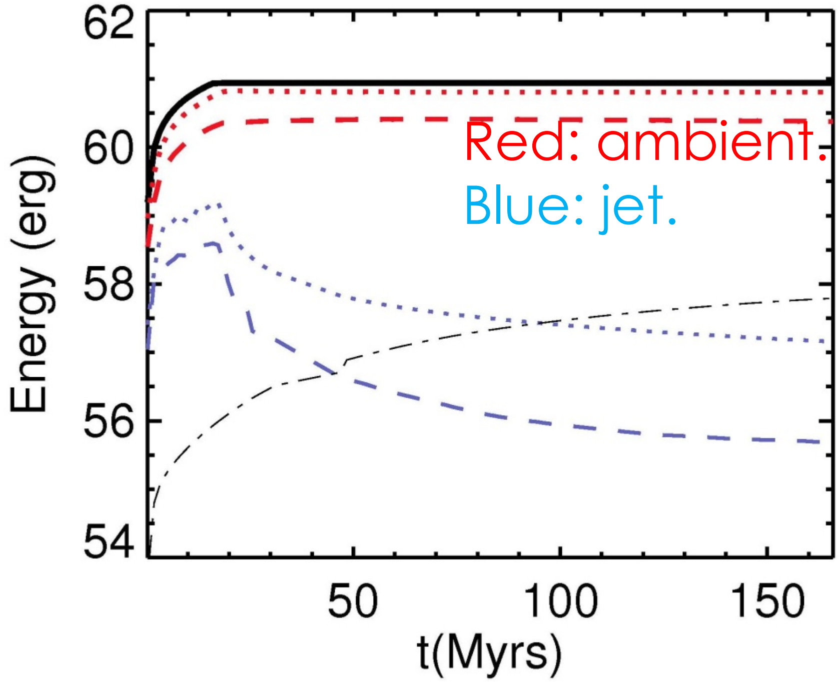

Up to 95 % or even more goes into the ambient medium via shock and mixing (≈ 1%).

10^{10} - 10^{11} $M_{\odot}$ of ambient gas are displaced by the shocks.

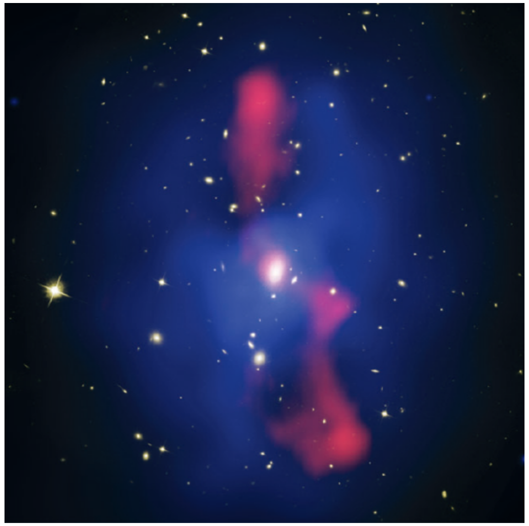

MS0735+7421 (McNamara et al. 2005).
Shock-wave (M=1.4).

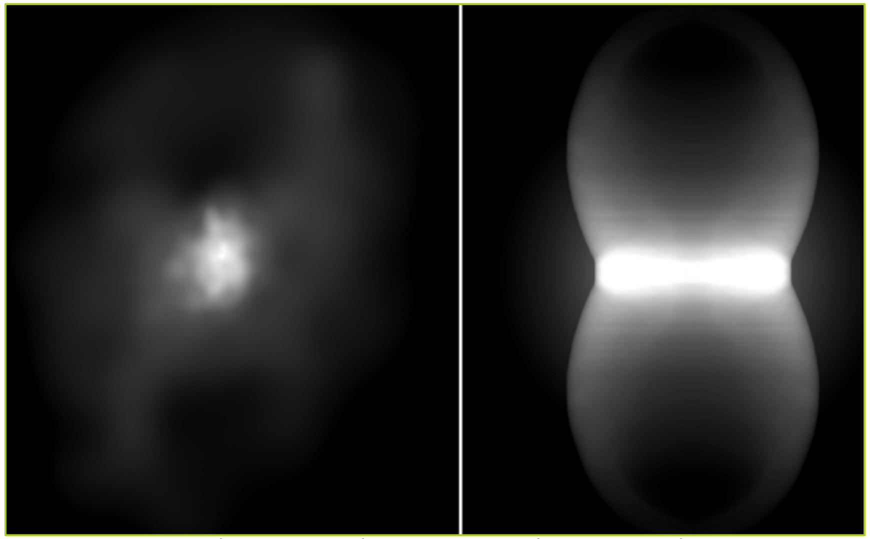

Comparison with our simulation J46

PKS B1358-113
(Stawarz et al.
2014).
Shock wave
(M ~ 2 - 4).

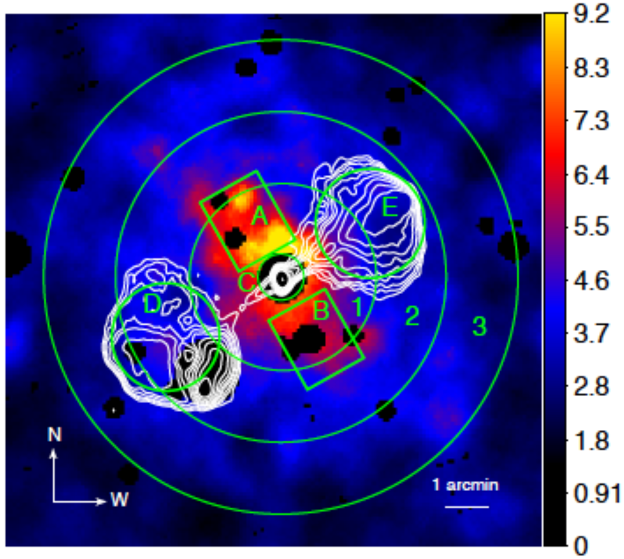

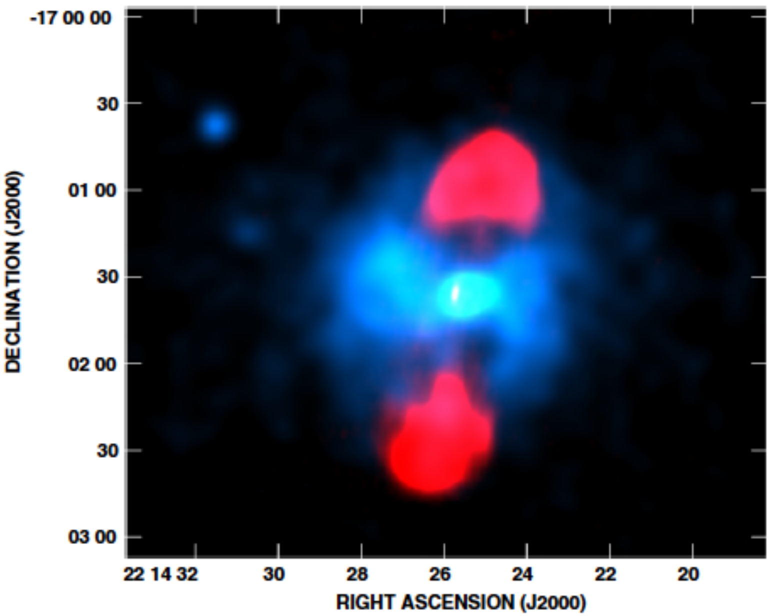

3C444 (Croston et al 2011).
Shock-wave (M=1.7).

Analytical models

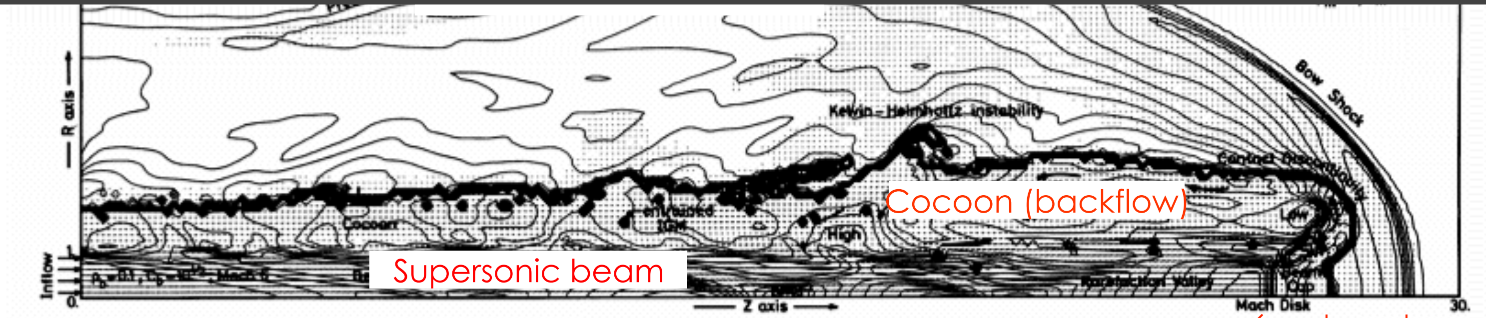

Head advance speed: 1D estimate from ram pressure equilibrium between jet and ambient in the rest frame of the jet working surface

relativistic jet

$$\rho_b h_b W_b'^2 v_b'^2 + p_b = \rho_a h_a W_a'^2 v_a'^2 + p_a \xrightarrow{v_{h,R} = -v_a'} \rho_b h_b W_b^2 (v_b - v_{h,R})^2 = \rho_a h_a v_{h,R}^2$$

$$v_{h,R} = \frac{\sqrt{\rho_b h_b W_b^2 / \rho_a h_a}}{1 + \sqrt{\rho_b h_b W_b^2 / \rho_a h_a}} v_b$$

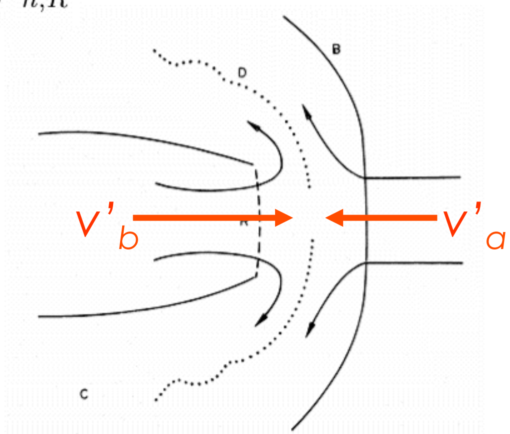

cf. classical

$$v_h = \frac{\sqrt{\rho_b / \rho_a}}{1 + \sqrt{\rho_b / \rho_a}} v_b$$

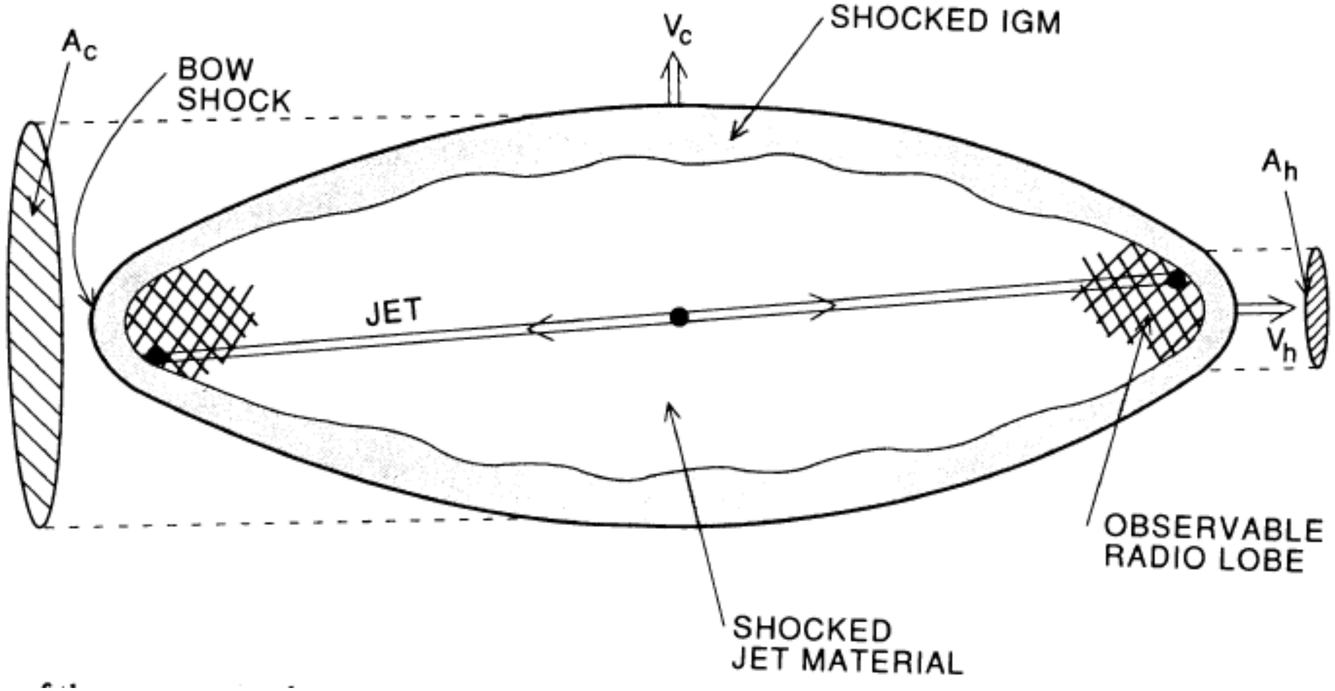

$$P_s \propto \frac{L_s}{v_{bs} A_s} \qquad \pi R_s^2,\ R_s \text{ being the radius}$$

$$P_s = \rho_a \dot{R}_s^2$$

$$\longrightarrow \quad 1/R_s \propto \dot{R}_s$$

strong shock limit

constant ambient density and bow-shock velocity variable velocity and density

$$v_{\rm c} \propto t^{\alpha},\ \rho_{\rm a} \propto r^{\beta} \qquad R_{\rm c} \propto t^{\frac{2-\alpha}{4+\beta}},\ P_{\rm c} \propto t^{\frac{2(\alpha-2)-\alpha(4+\beta)}{4+\beta}}$$

thermodynamical variables in the cocoon

$$P_{\rm c} \sim P_{\rm s} \propto \frac{L_{\rm s}}{v_{\rm bs} A_{\rm s}} \qquad \rho_{\rm c} = \frac{J_{\rm c}}{v_{\rm bs} A_{\rm c}} \qquad T_{\rm c} \propto \frac{L_{\rm s}}{J_{\rm c}} \frac{A_{\rm c}}{A_{\rm s}}$$

J_C : mass flux through the terminal shock (assumed constant)

$$\rho_c \propto t^{-1} \qquad T_c \propto t^0$$

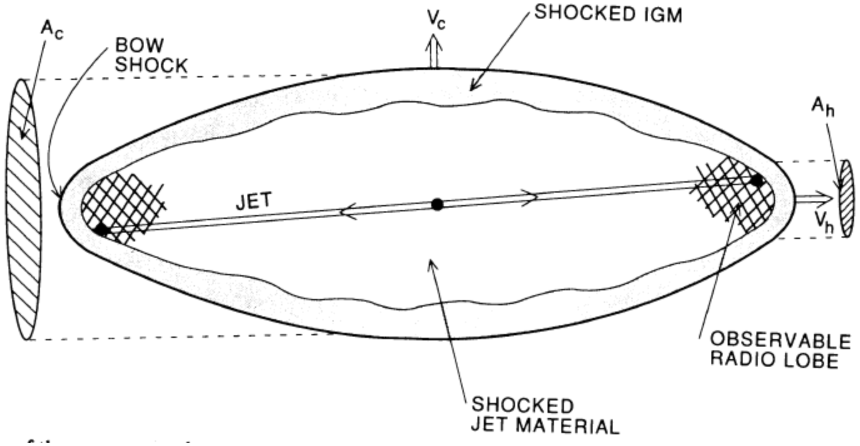

$v_c \propto t^{\alpha},\ \rho_a \propto r^{\beta}$ $\quad R_c \propto t^{\frac{2-\alpha}{4+\beta}},\ P_c \propto t^{\frac{2(\alpha-2)-\alpha(4+\beta)}{4+\beta}}$ $\quad R_c \propto t^{\frac{1-\alpha}{4+\beta}},\ P_c \propto t^{\frac{2(\alpha-1)-(1+\alpha)(4+\beta)}{4+\beta}}$

Active phase

Sedov phase

		1D phase				**2D phase**				**Sedov phase**			
		α	β	P_c	R_c	α	β	P_c	R_c	α	β	P_c	R_c
J1	Sim	0.07	-1.55	-1.58	0.75	-0.23	-0.52	-1.09	0.66	-0.74	-1.02	-1.70	0.90
	Model			-1.65	0.79			-1.05	0.64			-1.43	0.58
J2	Sim	0.27	-1.55	-1.67	0.67	-0.57	-0.52	-0.95	0.81	-0.83	-1.02	-1.67	0.72
	Model			-1.68	0.71			-0.91	0.74			-1.40	0.61
J3	Sim	0.13	-1.55	-1.55	0.67	-0.35	-0.52	-1.08	0.74	-0.60	-1.02	-2.16	1.00
	Model			-1.66	0.76			-1.00	0.68			-1.47	0.54

To be compared with Kawakatu, Nagai & Kino (2008): acceleration at the transition.
See Maciel & Alexander (2014)!! (Includes a study of the radiative evolution of radio-sources).

Conclusions

- Jet power, environment properties (including stellar population) seem to determine the evolution of radio-sources.
  - The possibilities are very diverse: There seems to be a continuous distribution of evolutionary tracks, more than a discretized set of possible evolution scenarios.
- Homework:
  - Simulations: The first stages of jet evolution, including effects on star formation rates of the host-galaxy, the role that magnetic fields play in jet dynamics,…
  - Population studies and observational studies: More studies of the relation of radio-sources and their environments, intermittent activity, polarization,…

Evolution on the P-D map

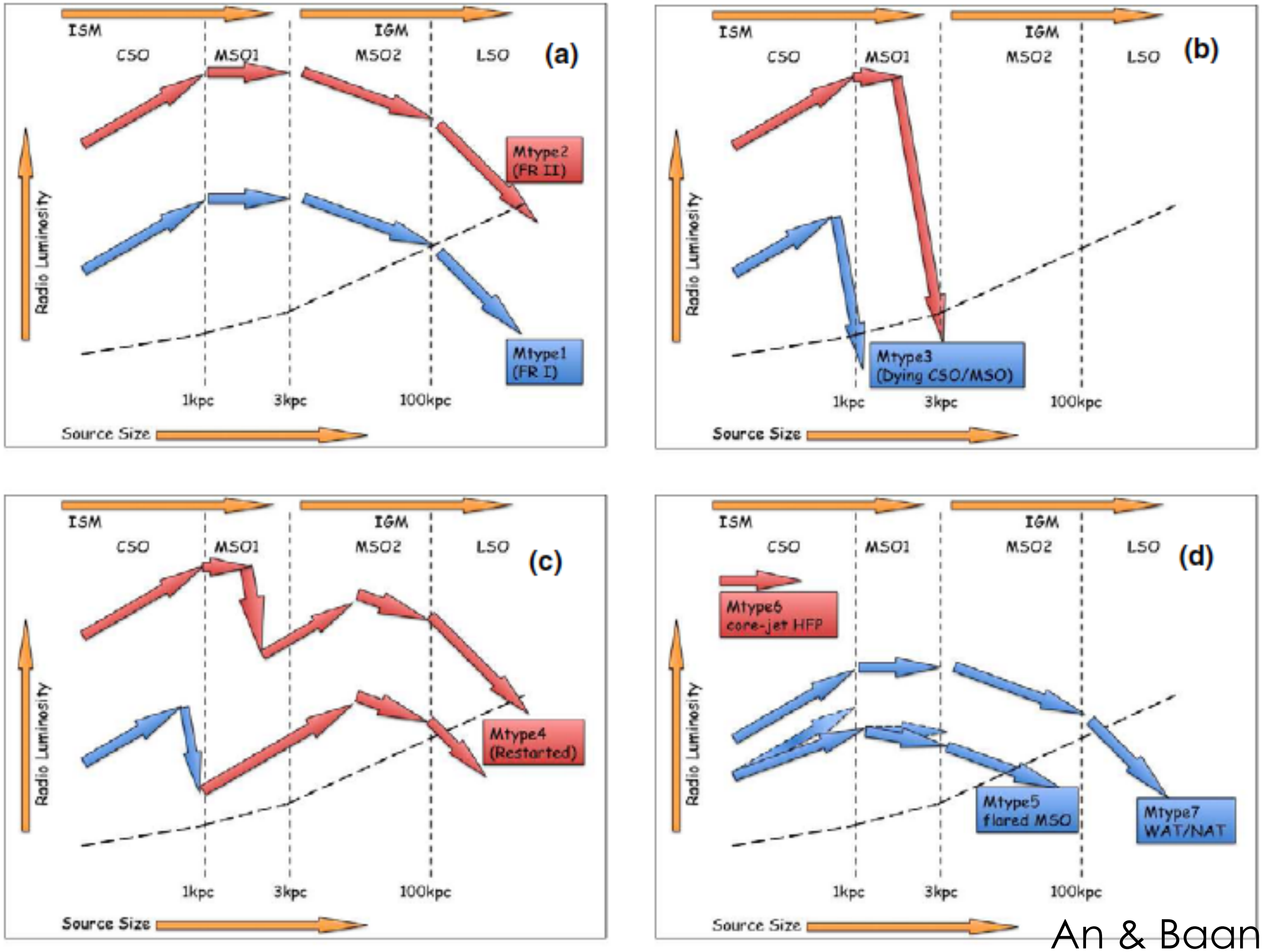

An & Baan 2012

Reactivation of radio-sources?

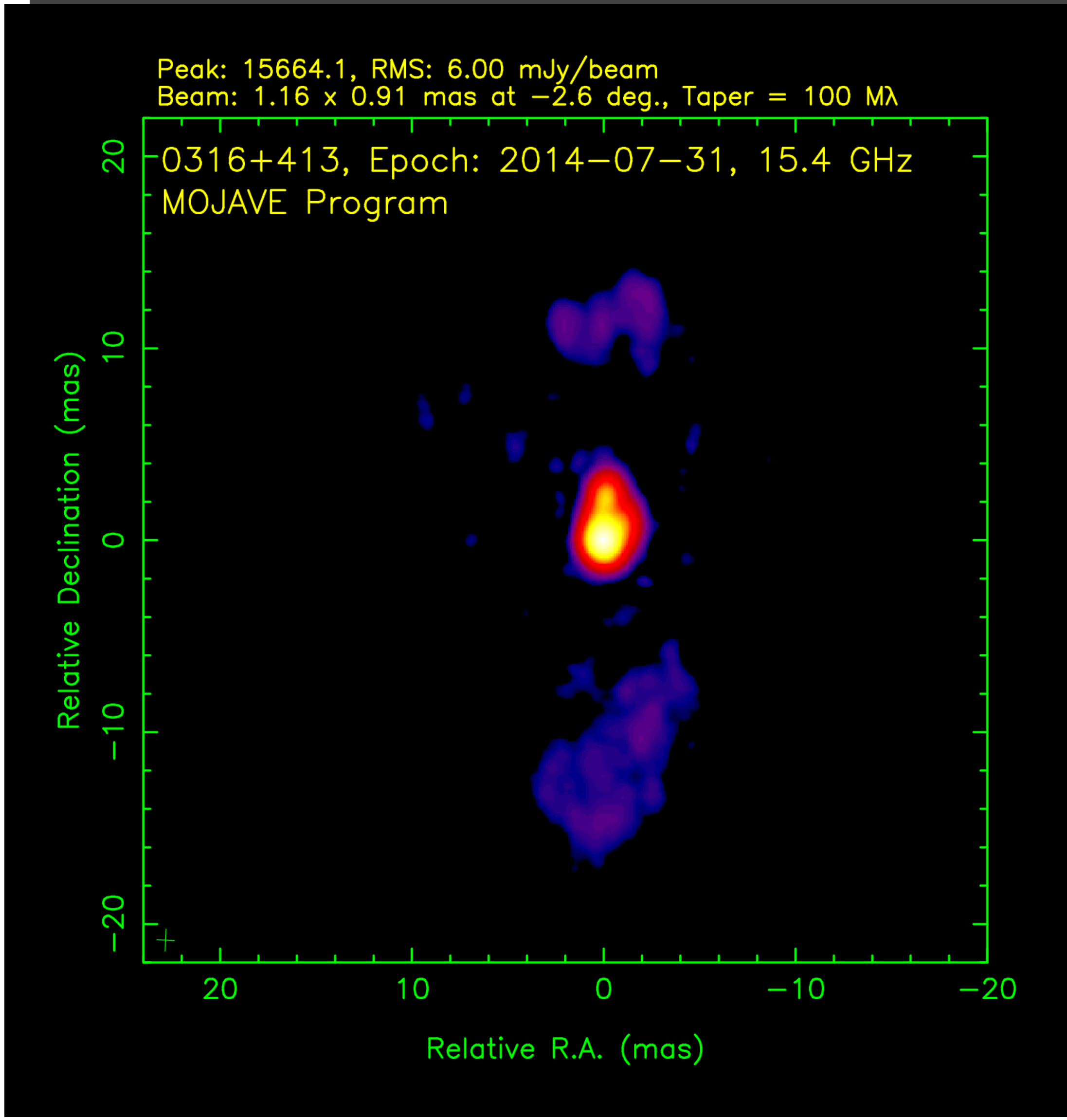

MOJAVE (15 GHZ) image of 3C84.

The tick marks are in 1 mas.

Reactivation of radio-sources?

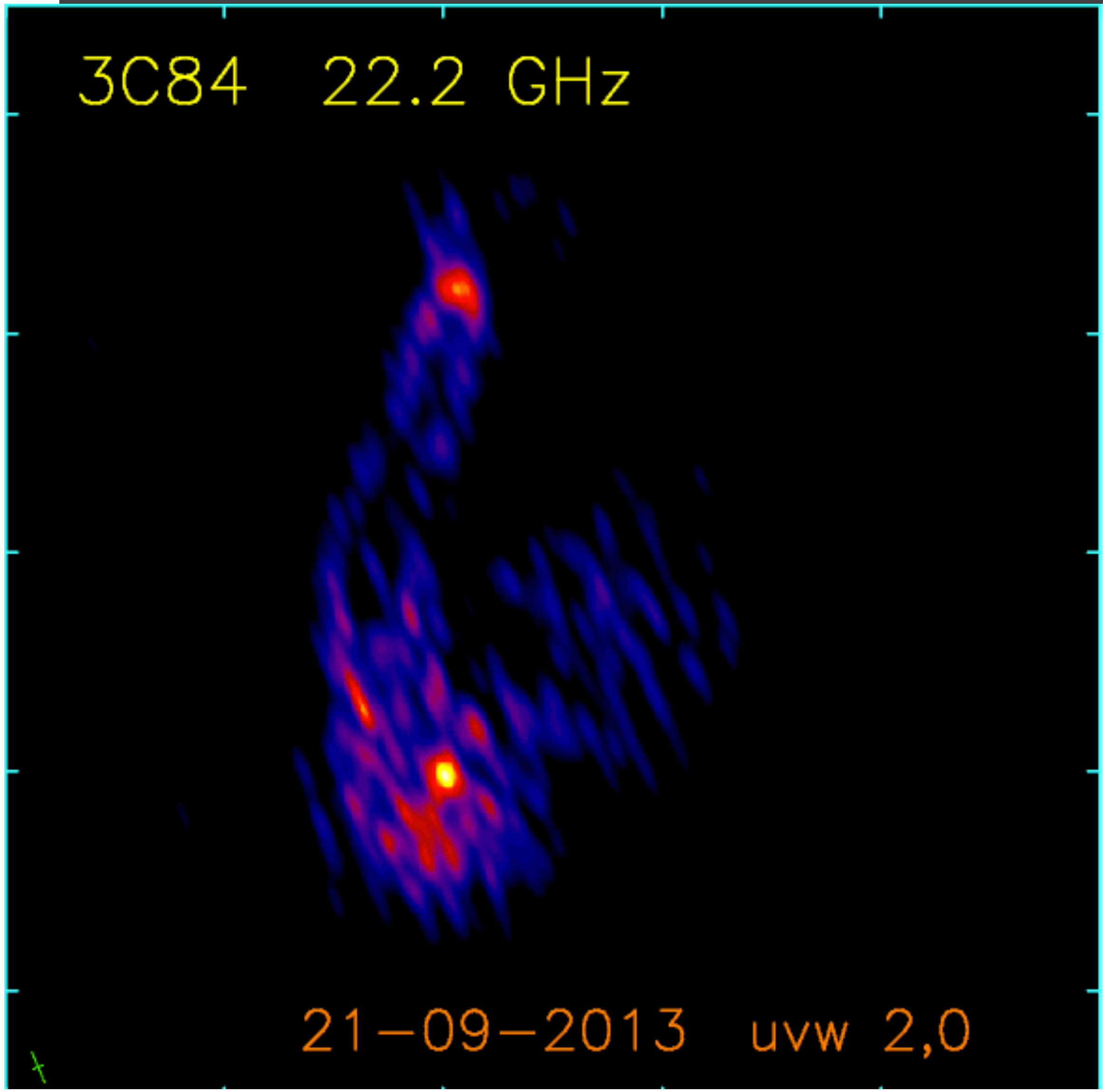

Radioastron image of 3C84

The tick marks are in 1 mas.

Savolainen et al. (in prep.)

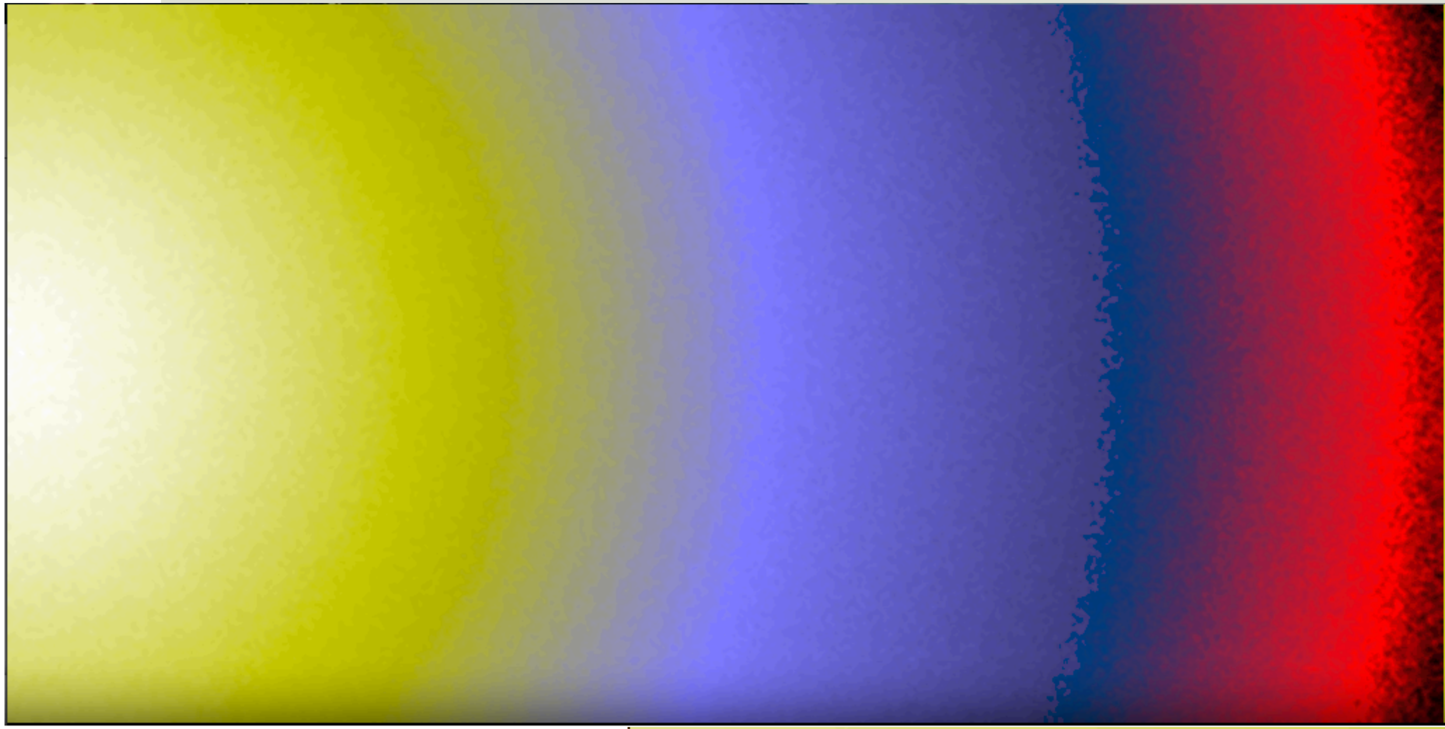

We are running 3D simulations of this scenario at Mare Nostrum (Barcelona Supercomputing Centre). These simulations include cooling terms and inhomogeneous ambient.